Xie *et al. Bioresour. Bioprocess. (2018) 5:21*
https://doi.org/10.1186/s40643-018-0208-6

Bioresources and Bioprocessing

RESEARCH

Open Access

Transcriptomic analysis of *Aspergillus niger* strains reveals the mechanism underlying high citric acid productivity

Hui Xie[1,3], Qinyuan Ma[2], Dong-Zhi Wei[1] and Feng-Qing Wang[1*]

Abstract

Background: *Aspergillus niger* is a highly important industrial microorganism because of its amazing capacity to produce citric acid (CA). To explore the metabolic mechanism and physiological phenotype associated with high CA productivity, the transcriptomes of high CA-producing *A. niger* YX-1217 and degenerative strain YX-1217G were investigated using *A. niger* ATCC1015 as a control.

Results: These strains showed distinct transcriptional differences in CA production. By contrast, the genes encoding glycoside hydrolases, aspartyl endoproteases, and carboxypeptidases were unusually upregulated in CA-producing strain YX-1217, which involved the carbohydrate hydrolysis and polypeptide degradation pathways, and should be related to its powerful capacity to utilize cornmeal fluidified liquid as raw material for the production of CA. In central metabolism of YX-1217, gene 9.735.1, which encodes glyceraldehyde 3-phosphate dehydrogenase, and two transcriptionally outstanding genes, 6000119 (An15g01920) and 3.2152.1 (An08g10920) that encode citrate synthase, were upregulated, thereby ensuring CA accumulation. In addition, a relatively strong electron transport chain, a regeneration system for NAD^+/$NADP^+$, and an efficient resistance mechanism may have contributed to the high CA production rate of YX-1217.

Conclusions: These comparisons have shed light on the mechanism underlying high CA yield in *A. niger* YX-1217 as well as provide insights into the development of novel strains that produce other organic acids.

Keywords: Transcriptome, *Aspergillus niger*, Citric acid, Metabolism

Background

Aspergillus niger is a ubiquitous fungus with powerful metabolic capabilities for the hydrolysis of carbohydrates and the production of organic acids and proteins. It has therefore been widely used as an industrial workhorse to commercially produce organic acids such as citric acid (CA) and gluconic acid, as well as industrial proteins such as enzymes and active proteins (Krijgsheld et al. 2013; Andersen et al. 2008). Along with advances in metabolic engineering and synthetic biology, *A. niger* has been highly studied to be developed as a more versatile cell factory platform.

As an important food additive and bulk chemical, CA has a long and successful production history by fermentation. Global CA production is more than 1.5 million tons per year, of which 99% comes from the fermentation of *A. niger*. The biochemical mechanism underlying the accumulation of CA in *A. niger* has recently been a research topic of great interest. In 2006, the US Department of Energy Joint Genomics Institute (JGI) completed the genome sequence of CA-producing *A. niger* ATCC 1015. Soon thereafter, as a powerful industrial enzyme producer, the genome of *A. niger* CBS513.88 was also sequenced and analyzed by DSM Food Specialties in 2007 (Pel et al. 2007). Currently, the genomes of at least four *A. niger* strains have been sequenced. Some

*Correspondence: fqwang@ecust.edu.cn
[1] State Key Lab of Bioreactor Engineering, Newworld Institute of Biotechnology, East China University of Science and Technology, Shanghai 200237, China
Full list of author information is available at the end of the article

metabolic network models of *A. niger* in genome scales have been established based on these sequences and used in the elucidation of the mechanism underlying CA production (Sun et al. 2007). The identified genes involved in CA metabolism and transport provide excellent opportunities to study and understand the mechanism of high CA production. The genome comparison of *A. niger* ATCC 1015 and CBS 513.88 has revealed genetic differences, particularly in relation to electron transport, carbohydrate transport, and organic acid transport, which in turn can shed light on the metabolic complexity relating to CA production (Andersen et al. 2011). Although extensive genomic studies have been conducted with *A. niger*, investigations relating to metabolic differences associated with variations in CA productivity among *A. niger* strains are still limited.

Recently, transcriptomics and proteomics studies on *A. niger* have revealed some distinct metabolic profiles at specific physiological statuses, such as the dormancy and germination stages of conidia (van Leeuwen et al. 2013). The RNA profile of dormant conidia is largely related to genes involved in fermentation, gluconeogenesis, and the glyoxylate cycle, whereas the profile at germination stage of conidia is associated with genes that are related to the metabolism of internal storage compounds (Novodvorska et al. 2013). Both researches clearly illustrate that transcriptional changes directly reflect the metabolic and physiological status of cells, and the observed major changes indicate cellular responses to alterations in the environment. The hydrolase secretory capacity of *A. niger* was also investigated by comparing transcriptomes in response to different carbon sources such as xylose or maltose, which revealed the transcriptional regulation profile of the secretory pathways and reflected a general modulation mechanism on the secretion capacity of extracellular hydrolases in *A. niger* (Jørgensen et al. 2009). Subsequently, proteomic analysis demonstrated that different carbon sources result in the production of specific extracellular enzymes such as glucoamylase A in response to D-maltose, and β-xylosidase in response to D-xylose (de Oliveira et al. 2011). These two studies have improved our understanding of the secretion capacity of *A. niger*. In addition, a more comprehensive study has analyzed the response of *A. niger* to carbon starvation in terms of changes in the physiological processes, morphological features, and genome-wide transcription (Nitsche et al. 2012). Although the metabolic properties of *A. niger* at different physiological statuses have been extensively studied using transcriptomics or proteomics approaches, to our best knowledge, no investigation has examined the metabolic mechanism underlying high CA productivity in *A. niger.* As the production of CA in the industry using *A. niger* is of significant economic value, understanding the complex mechanism underlying its production using omics approaches is essential.

China is the largest producer of CA, having more than 70% of the worldwide market share, the competitiveness of which benefits from the robust strains used in China with powerful CA productivity (> 150.0 g/L) from low-cost raw materials such as cornmeal, cassava, sweet potato, and other starch-rich crops. *A. niger* ATCC 1015 is a wild-type strain used in the first patented process for CA production nearly 90 years ago, which usually utilizes monosaccharides or disaccharides as raw materials and can only produce 10–20 g/L CA in 150 h at 30 °C. Obviously, the strains derived from *A. niger* ATCC 1015 or similar strains are hard to compete with the strains used in China in terms of productivity and production cost.

Aspergillus niger YX-1217 is a typical CA-producing strain used in the industry in China. Compared to *A. niger* ATCC 1015, it uses cornmeal as a raw material, producing 180–200 g/L CA in 55 h at 38–39 °C. Unfortunately, *A. niger* YX-1217 is not a genetically stable strain and is prone to spontaneous degeneration of CA production. To maintain its high CA-yielding phenotype, the strain must be regularly rejuvenated; otherwise, it would be degenerated to a low CA-producing strain (designated as YX-1217G) with an approximately 70% decrease in the CA production capacity compared to strain YX-1217.

To explore the metabolic profile and physiological phenotype associated with high CA yield, the transcriptomes of *A. niger* YX-1217 and YX-1217G were compared and analyzed in this study, and the transcriptome of *A. niger* ATCC1015 was used as a control. A comprehensive analysis of significant differences involved in CA production among these three strains identified events that were responsible for high CA yield in *A. niger* YX-1217, as well as provided novel insights into the development of strains that yield higher levels of CA or other organic acids.

Methods

Strains and growth conditions

Aspergillus niger YX-1217, YX-1217G, and ATCC 1015 were used in this study. For spore isolation, strains were grown for 7 days at 35 °C on sweet potato powder medium, and conidia were harvested and washed with a sterile detergent solution containing 0.05% (w/v) Tween-80 and 0.9% (w/v) NaCl. To this end, the colony surface was gently rubbed with a sterile T-spatula, and the conidial suspension was filtered through sterile glass wool and maintained at 4 °C until further analysis.

Sweet potato powder medium

Approximately, 250 g sweet potato powder was added to 1 L of water, stirred after adding 10 mL of high-temperature α-amylase, and liquefied for 40 min at 90 °C and then

measured by Brix. When the sugar content was adjusted to 6 Brix, the liquid was supplemented with 2% agar and 0.08% (w/v) of $(NH_4)_2SO_4$.

Cornmeal seed medium

Approximately, 250 g cornmeal was added to 1 L of water, stirring after continuously adding high-temperature α-amylase, and liquefied at 105 °C. Until the result of the iodine indicator test had no blue color, 20% (w/v) of cornmeal fluidified liquid was obtained. The liquid was filtered through two layers of gauze and used as seed medium.

Cornmeal fermentation medium

The filtered and unfiltered cornmeal fluidified liquid was mixed at a volume ratio of 6:1. The mixed liquid was then used as fermentation medium.

An aliquot of 3×10^8 conidia was added to 50 mL of the seed medium in a 250 mL Erlenmeyer flask. The cultures were shaken at 300 rpm and 35 °C for 33 h and then the seed liquid was inoculated into the fermentation medium at a concentration of 5% (v/v). Under the same conditions, the fermentation broth was cultured for 60 h. Each treatment was performed in triplicate.

Measure of CA and oxalic acid (OA) concentrations

CA and OA concentrations were determined using a high-performance liquid chromatography (HPLC) instrument equipped with a refractive index detector (RID), Aminex HPX-87H column (7.8 × 300 mm, Bio-Rad, California, USA) were used for CA and OA analysis. The eluent used for analysis was 0.01 N sulfuric acid solution. HPLC analyses were conducted under the following conditions: pump flow, 0.6 mL/min; column temperature, 40 °C; sample amount, 20 mL; and integration method, peak area. The concentrations were automatically calculated by Gilson Unipoint software.

Measurement of reducing sugar concentration and biomass

Reducing sugar concentrations were measured using an HPLC Dionex P 680 system with the following components: column type: Waters Xbridge Amide 3.5 μm 4.6 mm × 250 mm; detector: Shodex RI-101; injection volume: 20 μL; column temperature: 35 °C; flow rate: 0.8 mL/min; mobile phase: (acetonitrile:water ratio, 80:20).

To determine biomass production, wet fungal biomass that was collected after 60 h of growth was placed in a pre-weighed beaker and dried at 105 °C to a constant weight. Biomass levels are expressed as grams of cell weight per milliliter of fermentation broth. All values represent the mean of three independent determinations where the experiments were performed in triplicate.

RNA extraction

Conidia (10^8/mL) were germinated in the seed media for 10 h at 35 °C. The pellets were cultured in the fermentation media for 40 h at 35 °C. Germinating conidia and pellets were centrifuged at 6000 rpm for 20 min and then immediately frozen in liquid nitrogen and stored at − 80 °C for RNA extraction.

For Illumina sequencing, total RNA was extracted from germinating conidia (10 h) and pellets (40 h) using TRIzol reagent (Invitrogen, Carlsbad, CA, USA) according to the manufacturer's instructions. To maximize target coverage, equal amounts of total RNA (10 μg) from three independent RNA extractions were pooled for RNA-Seq library construction at each time point. The concentration and quality of RNA for each sample were determined by UV spectrometry (Agilent Technologies, Santa Clara, CA, US). Quality checks and subsequent RNA-Seq experiments were performed at the Next Generation Sequencing Facility (Shanghai Biotechnology Corporation, China).

Construction of cDNA library and transcriptome data analysis

The cDNA library was sequenced using the Illumina HiSeq 2000 with a paired-end 2 × 100-nt multiplex with two separate technical replicates. Clean reads were obtained by removing raw reads that contained the adaptor, unknown, or low-quality sequences. Clean reads were mapped to the genome sequence assembly of *A. niger* strain ATCC 1015. Full sequences and annotations are available from the Joint Genome Institute (JGI) Genome Portal (http://genome.jgi-psf.org/Aspni5). To ensure the most comprehensive gene model possible, clean reads were also mapped to the genome sequence assembly of *A. niger* CBS 513.88 genome from NCBI. The appendix file linking the CBS 513.88 annotation to ATCC 1015 annotation is presented in Additional file 1: Table S1. LifeScope provided all read alignment positions of each paired-end reads mapped against the complete genome sequence and exon spanning junctions. The read alignment results were recorded in BAM format for further downstream analysis. Read counts per gene were determined from primary read alignments with a mapping quality of ≥ 20 (MAPQ20). These counts were then used to calculate normalized expression values of fragments per kilobase of exon model per million mapped reads (FPKM) for each gene, as well as an input for determining significantly differentially expressed genes. BAM files were used as input, opting to ignore or include strand specificity in the calculations. Data were visualized

using Integrative Genomic Viewer (IGV). Differentially expressed genes were screened using a false discovery rate (FDR) of ≤ 0.05, an absolute value of the $\log_2$ ratio of ≥ 1, and an FPKM ≥ 50 in strain YX-1217 at stage 10 h or stage 40 h as threshold. In addition, the genes that have small differences but have a decisive impact on CA production were included in the analysis.

To predict the cellular and metabolic functions associated with the observed changes in transcript levels, differentially expressed genes selected were categorized according to predicted protein function using the Kyoto Encyclopedia of Genes and Genomes (KEGG) database (http://www.genome.jp/kegg/).

Real-time quantitative RT-PCR (qRT-PCR) analysis

To validate our RNA-Seq results, the transcript expression of eight genes related to the CA metabolism was verified by qRT-PCR and reverse transcribed into cDNA by PrimeScriptH RT reagent kit with gDNA Eraser (Takara, Japan). qRT-PCR was performed using a Bio-Rad CFX-96 Real-Time PCR System (Bio-Rad, California, USA) with a final volume of 20 μL containing 2 μL of cDNA template, 10 μL of 26SYBR premix ExTaq™ (Takara, Japan), 1 μL of each forward and reverse primer (10 mM) (Additional file 2: Table S2), and 6 μL of RNase-free water. Gene transcription was analyzed using SYBR green assays as previously described (Steiger et al. 2009).

Results and discussion

Performances of *A. niger* YX-1217, YX-1217G, and ATCC1015

After several subcultures, some of the strains that germinated from the conidia of *A. niger* YX-1217 spontaneously degenerated into low CA-yielding strains. These degenerate strains exhibited no significant differences in growth and could maintain genetic stability in further multiple subcultures. Therefore, a degenerate strain YX-1217G was randomly selected for comparison with strain YX-1217 to explore genomic variations between high and low CA-yielding strains.

The variations in growth phenotypes and production performances between *A. niger* YX-1217 and YX-1217G were first investigated by using *A. niger* strain ATCC1015 as a control. These strains were all cultivated in the same conditions using cornmeal fermentation broth as medium and culturing at 35 °C for 60 h. After 60 h of fermentation, biomass, reducing sugars, and CA and OA concentrations of the three *A. niger* strains were measured (Table 1). The CA concentration of the three strains consistently increased with fermentation time (Fig. 1).

Apparently, strain YX-1217 is a robust CA-producing strain that could reach the highest CA titer of 180.0 g/L at 60 h with 3.0 g/L/h productivity, whereas the degenerate strain YX-1217G could only reach 65 g/L and 1.1 g/L/h productivity, indicating an almost 70% decrease in CA production capacity compared to strain YX-1217. Strain YX-1217 produced approximately 120 g/L CA more than YX-1217G, while producing approximately 15.1 g/L less biomass. For strain YX-1217G, the more the biomass, the less was the CA yield, which signified that part of the attenuated metabolism of CA production had shifted to the growth of *A. niger*. In addition, strain YX-1217 could only produce 0.89 g/L OA at 60 h, whereas strain YX-1217G had a yield of 5.78 g/L OA, which indicated that the degeneration involved not only CA metabolism but also that of other organic acids.

As *A. niger* YX-1217G is a degenerated strain of *A. niger* YX-1217 in terms of CA production, the close correlation between the two strains makes them good comparison objects to analysis some of the high yield mechanisms of CA by comparative omics. Considering that *A. niger* ATCC 1015 is a typical CA-producing strain and often employed as a representative research model for CA overproduction (Pel et al. 2007; Andersen et al. 2011), this strain is also selected as an available reference to analyze the distinctive feature of *A. niger* YX-1217 relating to the yield of CA. Experimental results show that all of the three strains can employ diverse carbohydrate-containing materials to produce CA, including cornmeal fluidified liquid. By contrast, the CA production capacity of strain ATCC1015 was significantly lower than that of strains YX-1217 and YX-1217G in the condition of 35 °C and 60 h, which reached only 20.0 g/L and 0.33 g/L/h CA productivity. As CA production of the strain ATCC 1015 was evaluated by glucose, it was tested in a glucose-based minimal medium, which only achieved 0.10 ± 0.12 g/L CA (Andersen et al. 2011). Briefly, the productivities among these strains are significantly different, and thus are good samples to explore the mechanism underlying high CA yield in *A. niger* by a comparative omics approach.

Transcriptional profiling

To directly demonstrate metabolic variations among these strains, transcriptomics analysis was utilized in mRNA expression profiling in relation to high CA yield. Cultures at the two different stages of each strain were selected and used in transcriptomics analysis. One stage was conidial germination, which was sampled from the seed medium cultured for 10 h, as the conidial germination of these *A. niger* strains was observed to flourish at 10 h, and it was reported that the majority of transcriptomic changes occur early during the germination phase (Novodvorska et al. 2013). Furthermore, at this stage, the nutrient content and pH of the medium do not undergo significant changes. More importantly, this stage involves

the initial production of CA once germs emerge on the conidia, which was subsequently followed by the fast CA-producing period, signifying that CA metabolism has entered the active phase. It is thus the appropriate and reliable time point to compare metabolic differences at the initial stage of CA production among these strains. The other stage was the high CA yield phase, which involves culturing in fermentation medium for 40 h (Fig. 1). At this stage, these strains are all at their peak phase of CA production and exhibit significant differences in CA titer, intracellular metabolic activities, CA tolerance, and other aspects closely related to high CA yield capacity. Because the nutrients in the medium have not been depleted during metabolism among the three strains, the differential data at this stage may be usable in profiling CA yield in *A. niger* YX-1217.

Global transcriptional profiles of the three samples at two different phases were established using RNA-Seq. The number of clean reads and mapping ratio are presented in the supplemental material (Additional file 3: Table S3), and the mapping ratios were all more than 90%, which suggests that sequencing was sufficient. The comparison of strain YX-1217 to strain ATCC 1015 (designated as *S*1/*S*3) indicated 1020 upregulated genes (Additional file 4: Table S4) and 1084 downregulated genes (Additional file 5: Table S5) during the conidial germination stage (10 h) and 1058 (Additional file 6: Table S6) upregulated genes and 3024 downregulated genes (Additional file 7: Table S7) at the high citric acid yield stage. The comparison of strain YX-1217 with strain YX-1217G (designated as *S*1/*S*2) showed 506 upregulated genes (Additional file 8: Table S8) and 356 downregulated genes (Additional file 9: Table S9) during conidial germination and 1206 upregulated genes (Additional file 10: Table S10) and 1963 downregulated genes (Additional file 11: Table S11) during high CA yield. The global gene expression profiles (scatter plots) of various samples are shown in Fig. 2.

Significantly greater transcriptional differences between *A. niger* YX-1217 and ATCC 1015 compared to that between *A. niger* YX-1217 and YX-1217G at the same stage were observed, and there were abundant genes that were more than tenfold up- or downregulated in the former stage than in the latter stage, which could be ascribed to their genetic relationship or their strain intrinsic physiological differences. This detailed analysis would provide an authentic view of the mechanism underlying high CA production.

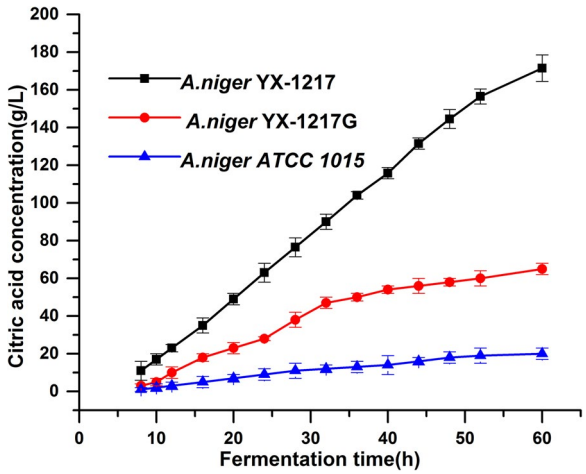

Fig. 1 Results of citric acid fermentation by the three *A. niger* strains. The curves indicate that the citric acid concentration of *A. niger* YX-1217, YX-1217G, and ATCC 1015 increased consistently with the fermentation time

Functional annotation of differentially expressed genes

Differentially expressed genes were functionally annotated to KEGG pathways to explore metabolic variations among different strains. The major KEGG pathways identified were associated with global metabolism, particularly CA biosynthesis that is related to starch and sucrose metabolism, glycolysis, TCA cycle, and fatty acid metabolism (Figs. 3 and 4).

Transcript abundance was higher in strain YX-1217 than in ATCC 1015 and YX-1217G during conidia germination, and in most of the categories the genes in strain YX-1217 were upregulated, except for those belonging to the categories of ribosomes, RNA transport, and

Table 1 Comparison of biomass, residual reducing sugars, citric acid, and oxalic acid concentration among the three strains at 60 h

Strains	Initial reducing sugars (g/L)	Biomass (g/L)	Citric acid concentration (g/L)	Oxalic acid concentration (g/L)	Residual reducing sugars (g/L)
A. niger YX-1217 (*S*1)	175.2 ± 2.5	132.4 ± 4.5^{C}	180.0 ± 0.1^{A}	0.89 ± 0.06^{C}	3.5 ± 0.5^{C}
A. niger YX-1217G (*S*2)	175.2 ± 2.5	157.5 ± 5.2^{B}	65.0 ± 0.1^{B}	5.78 ± 0.54^{A}	43.8 ± 1.0^{B}
ATCC 1015 (*S*3)	175.2 ± 2.5	192.5 ± 4.4^{A}	20.0 ± 0.05^{C}	1.83 ± 0.22^{B}	86.0 ± 1.2^{A}

Fermentations were performed in biological triplicate for each strain. Values are presented as the average ± standard deviation. For significance analysis, each column was listed as a level, and different uppercase letters represent extremely significant differences ($p < 0.01$)

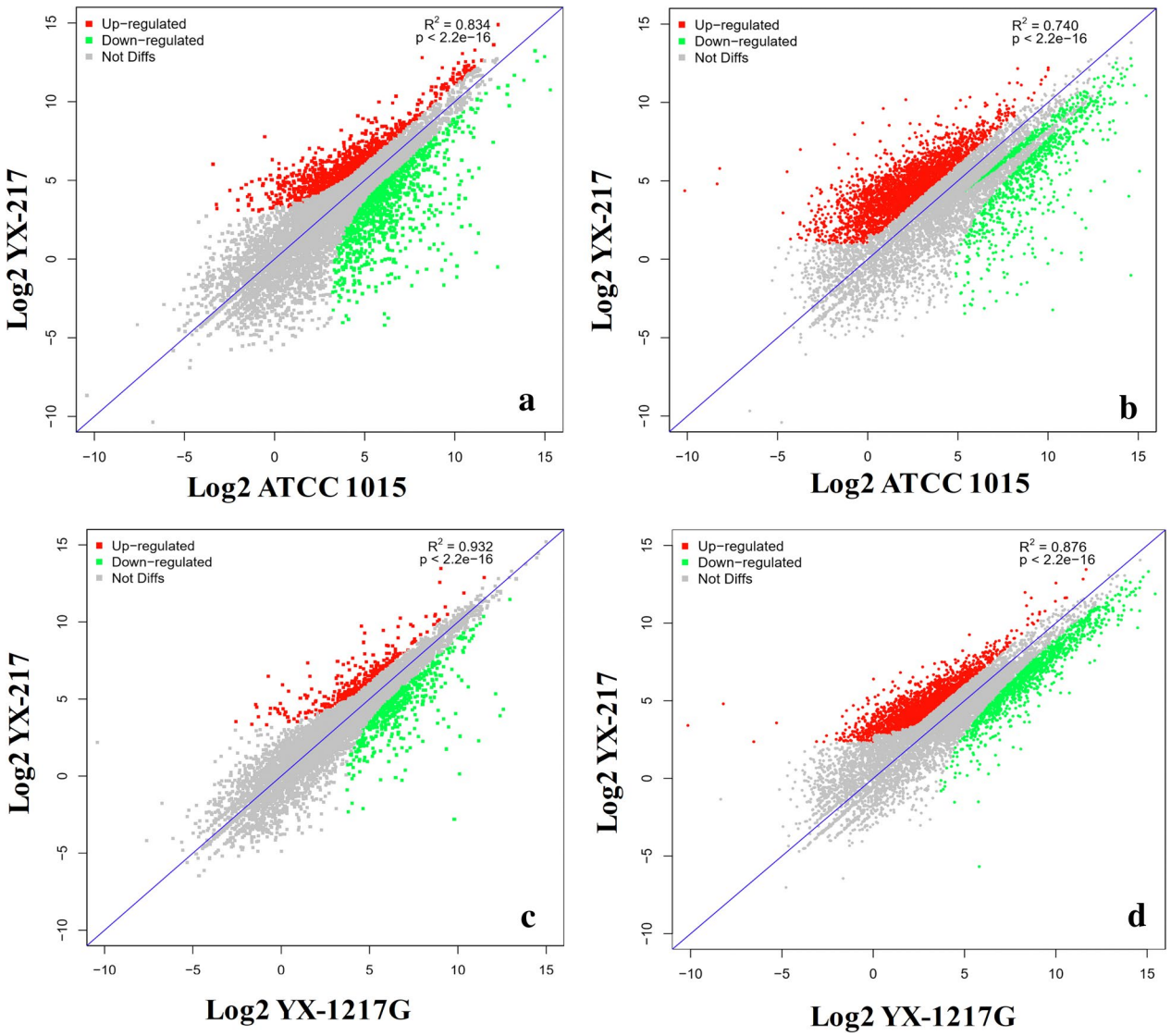

Fig. 2 Scatter plots of gene expression levels across different samples. **a** The transcriptional differences between *A. niger* YX-1217 and ATCC 1015 (*S*1/*S*3) at the stage of 10 h; **b** the transcriptional differences between *A. niger* YX-1217 and ATCC 1015 (*S*1/*S*3) at the stage of 40 h; **c** the transcriptional differences between *A. niger* YX-1217 and *A. niger* YX-1217G (*S*1/*S*2) at the stage of 10 h; **d** the transcriptional differences between *A. niger* YX-1217 and *A. niger* YX-1217G (*S*1/*S*2) at the stage of 40 h

amino acid biosynthesis, signifying that protein expression is not active in strain YX-1217 compared to strains ATCC1015 and YX-1217G. At the peak stage of CA production, most of the genes that are closely related to CA biosynthesis such as those of TCA cycle, starch and sucrose metabolism, glycolysis, and pyruvate metabolism were downregulated in strain YX-1217G compared to the other two strains. Notably, most of the ribosome-associating genes were upregulated in *S*1/*S*3 and *S*1/*S*2 at the peak stage of CA production (40 h), indicating that protein expression is higher in strain YX-1217 than the other strains at this stage.

To concretely distinguish the specific genes and possible mechanism contributing to high CA productivity, the genes belonging to the above categories at the two stages were further examined individually in the following sections using the selection criterion of FPKM $\geq$ 50 in strain YX-1217 at the stage of 10 or 40 h, $\log_2$ratio $\geq$ 1, and FDR $\leq$ 0.05.

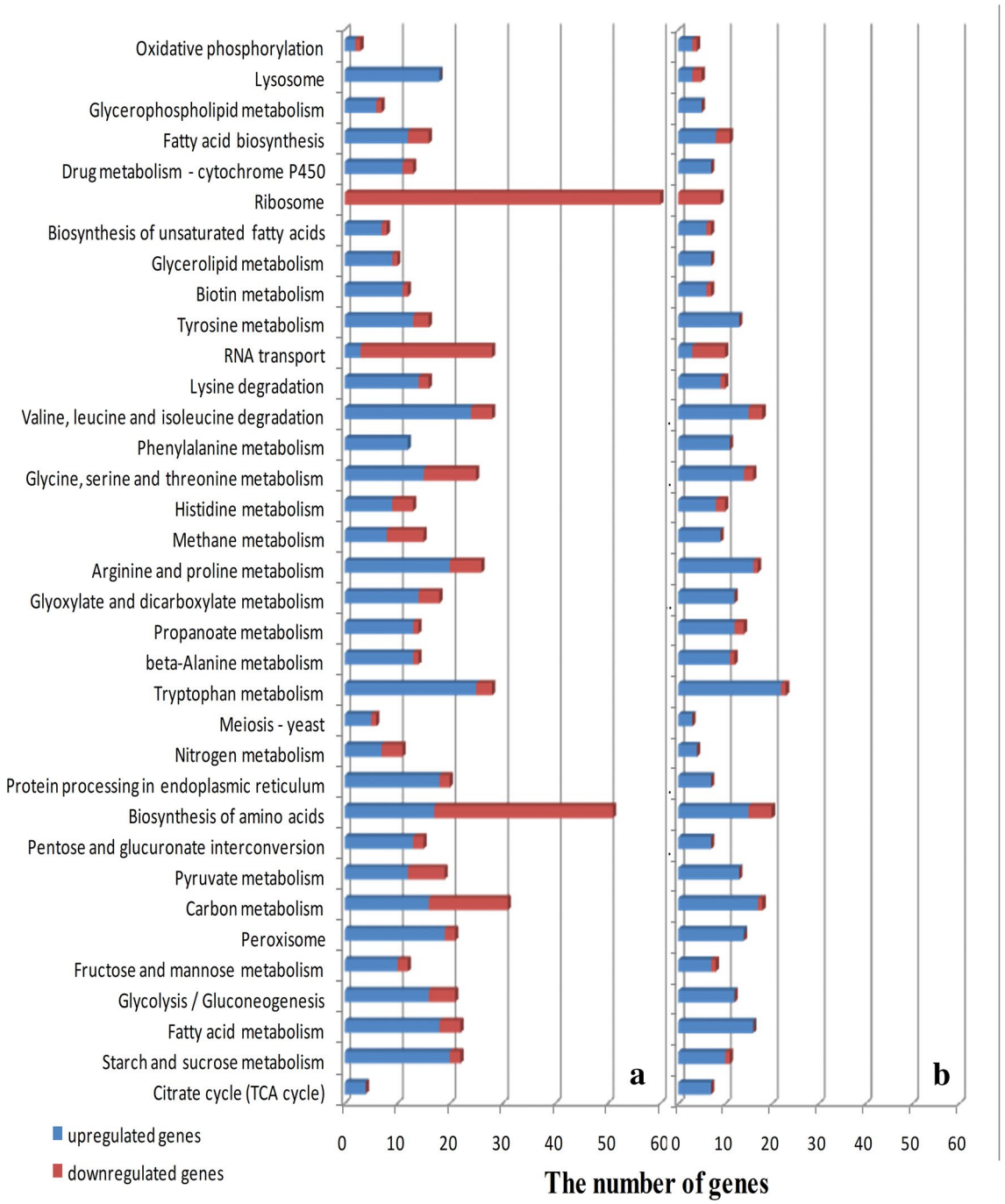

Fig. 3 Comparative transcriptomic data at the stage of 10 h clustered by KEGG categories. **a** Comparative transcriptomic data of strain YX-1217 versus ATCC 1015 (*S1*/*S3*) at the stage of conidia germination (10 h culture of conidia in seed medium) clustered by KEGG categories; **b** Comparative transcriptomic data of strain YX-1217 versus YX-1217G (*S1*/*S2*) at the stage of conidia germination (10 h culture of conidia in seed medium) clustered by KEGG categories

Regulation of carbohydrate hydrolysis among different *A. niger* strains

Utilization of a wide range of carbohydrates as carbon sources is an important feature of *A. niger*. In industry, cornmeal is often used as an inexpensive carbon source for the fermentation of *A. niger*, and strain YX-1217 is the typical CA-producing strain that can convert high Brix starch to CA. In the present study, transcriptional

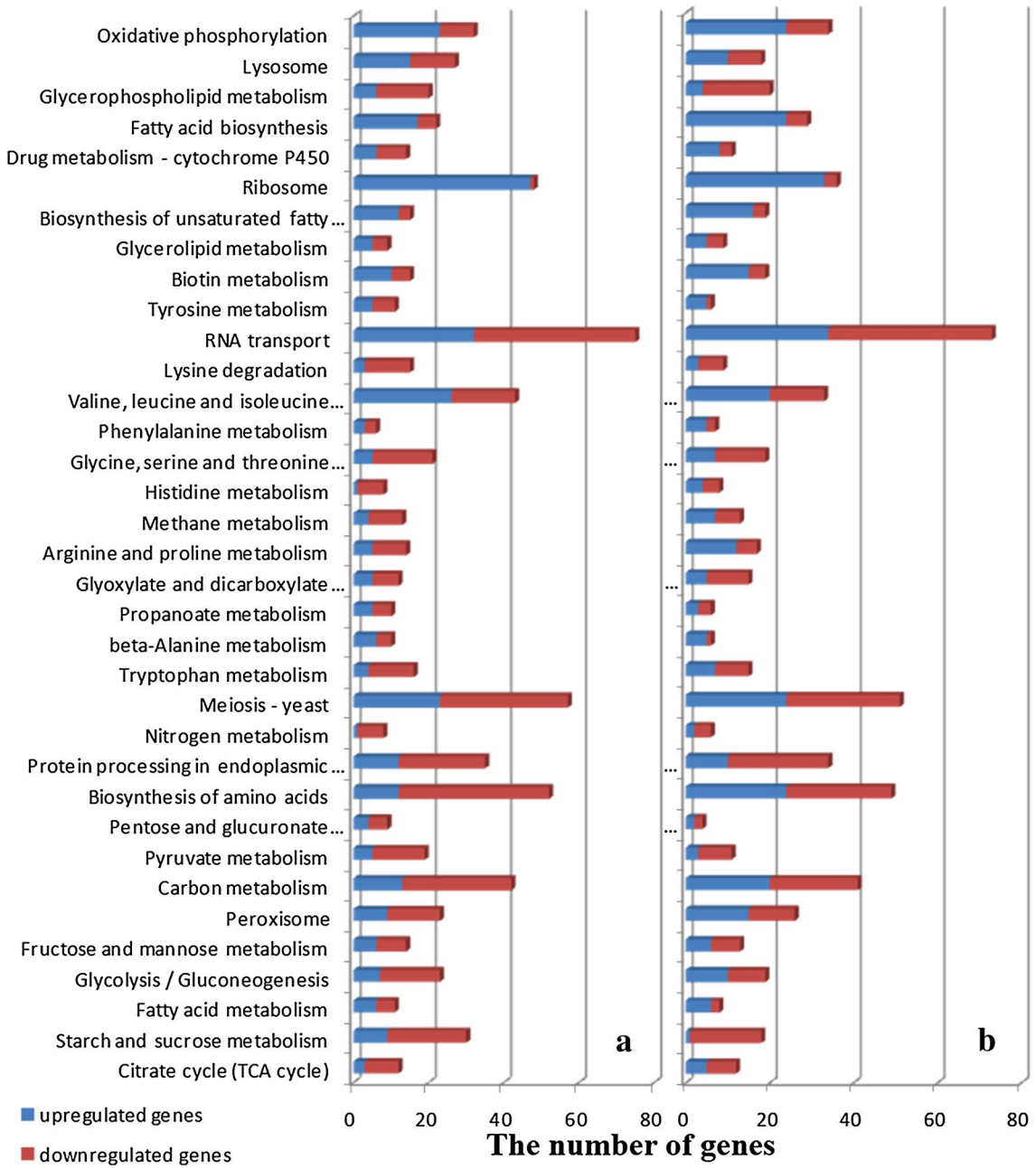

Fig. 4 Comparative transcriptomic data at 40 h clustered by KEGG categories. **a** Comparative transcriptomic data of strain YX-1217 versus ATCC 1015 (*S1*/*S3*) at the peak stage of CA production (40 h culture of CA fermentation) clustered by KEGG categories. **b** Comparative transcriptomic data of strain YX-1217 versus YX-1217G (*S1*/*S2*) at the peak stage of CA production (40 h culture of CA fermentation) clustered by KEGG categories

variations in hydrolases between strains YX-1217 and ATCC1015 and YX-1217G were first analyzed (Table 2).

The degradation of starch is performed by a variety of enzymes, which are divided over three glycoside hydrolase (GH) families based on their sequence similarity http://www.cazy.org), including GH13, GH15, and GH31 (Adav et al. 2010; Yuan et al. 2008). To date, several *A. niger* genes involved in extracellular starch hydrolytic enzymes have been characterized. GH13, a large family containing various hydrolyzing and transglycosylating enzymes, can mostly act on α-(1,4) or α-(1,6)-glycosidic bonds. GH31 releases glucose from the non-reducing end of starch. Here, the expression levels of genes *agsA* (An04g09890), *agdC* (An02g13240), *amyA*,

Table 2 Expression of genes involved in carbohydrate hydrolytic pathway

Gene ID (1015)	Gene ID (513.88)	Predicted function (homolog and organism)[a]	FPKM-10 h			FPKM-40 h			Fold change[b]			
			S1	*S3*	*S2*	*S1*	*S3*	*S2*	*S1*/*S3* (10 h)	*S1*/*S2* (10 h)	*S1*/*S3* (40 h)	*S1*/*S2* (40 h)
220039	An04g09890	*agsA*, GH13, alpha-amylase, alpha-1,3 glucan synthases	85.31	3.70	69.89	18.92	84.01	41.45	4.52	–	− 2.15	− 1.13
20924	An02g13240	*agdC*, GH13, alpha-amylase, (*A. parasiticus glcA*)	94.33	6.81	34.64	9.80	27.69	25.98	3.79	1.44	− 1	− 1,79
4000142	No	*amyA*, GH13, alpha-amylase, catalytic region	314.72	7.81	364.47	10,173.90	196.30	8128	5.33	–	5.69	–
6.225.1	An15g07800	*agtC*, GH 13, alpha-amylase, catalytic region	18.68	0.88	2.99	4.99	43.02	0.24	4.40	2.64		4.37
80803	An14g04190	*gbeA*, glycoside hydrolase GH 13, 1,4-alpha-glucan-branching enzyme	80.46	10.18	19.34	15.07	58.91	53.08	2.98	2.05	− 1.96	− 1.81
140568	An03g06560	Glycoside hydrolase GH15, glucan-1,4-alpha-glucosidase with starch-binding domain	2003.34	36.57	1922.03	7633.04	293.32	8669.53	5.77	–	4.7	–
1.137.1	An01g10930	*agdC*, glycoside hydrolase, GH31, alpha/beta-glucosidase	325.56	65.10	122.57	99.21	41.37	405.03	2.32	1.41	1.26	− 2.03
170127	An04g06920	*agdA*, glycoside hydrolase, GH 31, alpha-glucosidase	2116.14	213.84	860.88	1651.11	241.73	1790.41	3.30	1.29	2.77	–
180456	An16g06800	Glycoside hydrolase, GH 5, endoglucanase A	505.16	93.65	557.327	104.11	77.28	449.4	2.43	–	–	− 2.11
190032	An03g00940	Glycoside hydrolase, GH 10, endo-1,4-beta-xylanase F1	1100.38	0.45	1.12	108.75	1.64	18.16	11.24	9.96	6.05	2.58
11115	An01g00780	*xynB*, glycoside hydrolase, GH 11, endo-1,4-beta-xylanase	218.08	13.44	5.87	191.03	0.45	29.15	4.02	5.22	8.74	2.71
80523	An14g02760	*eglA*, glycoside hydrolase GH 12, endoglucanase A	460.75	1.92	10.67	85.96	4.34	375.94	7.9	5.43	4.3	− 2.12
10876	An01g03340	Glycoside hydrolase GH 12, xyloglucanase	25.10	7.61	52.69	255.83	6.47	47.62	1.72	− 1.05	5.3	2.42
6000593	An15g07760	Glycoside hydrolase, GH 26, mannan endo-1,4-beta-mannosidase E	316.29	62.32	63.14	11.45	1.10	9.46	2.34	2.32	3.37	–
22004	An02g11150	*aglB*, glycoside hydrolase, GH 27, alpha-galactosidase B	59.76	6.19	41.36	618.92	1.10	248.35	3.27	–	9.14	1.32
20338	An02g04900	Glycoside hydrolase, GH 28, endopolygalacturonase C	698.14	21.98	362.65	458.52	16.00	307.35	4.99	–	4.84	–
90046	An12g08280	*inuE*, glycoside hydrolase, GH 32, inulinase	224.97	14.74	52.39	8.03	0.50	3.50	3.93	2.1	4.01	1.19
17000028	An04g06990	Glycoside hydrolase, GH 47,1, 2-alpha-mannosidase	62.66	14.20	92.03	47.61	125.33	99.55	2.14	–	− 1.40	–
30627	An08g05230	Glycoside hydrolase, GH 61, endoglucanase-4	468.30	6.76	19.19	13.28	8.30	30.59	6.11	4.61	–	− 1.20
6.376.1	An15g04900	Glycoside hydrolase, GH 61, endo-beta-1,4-glucanase D	130.324	6.08	1.30	0.59	1.07	2.03	4.42	6.65	–	− 1.79

Table 2 continued

Gene ID (1015)	Gene ID (513.88)	Predicted function (homolog and organism)[a]	FPKM-10 h			FPKM-40 h			Fold change[b]			
			S1	*S3*	*S2*	*S1*	*S3*	*S2*	*S1*/*S3* (10 h)	*S1*/*S2* (10 h)	*S1*/*S3* (40 h)	*S1*/*S2* (40 h)
190140	An03g00960	*axhA*, Glycoside hydrolase, GH 62, alpha-L-arabinofuranosidase	648.17	1.98	3.37	563.18	1.59	66.70	8.36	7.59	8.47	3.08
210054	No	Chitinase	1761.52	48.82	494.28	513.94	728.75	1145.75	5.17	1.83	–	−1.15
10199	An01g12440	Chitin-binding, domain 3	367.96	15.93	29.17	333.84	7.89	39.68	4.52	3.65	5.4	3.07
140158	An03g04190	Chitinase	213.33	20.54	283.81	347.27	212.54	617.82	3.37	–	–	–
13.203.1	An04g04670	*cfcC*, GH18, Chitinase	150.49	18.23	56.79	96.25	162.39	119.70	3.04	1.4	–	–
10106	An01g12450	*bxgA*, chitinase	245.54	37.36	83.58	465.89	7.44	205.65	2.72	1.55	5.97	1.18
80155	An14g01840	Chitinase	494.65	192.43	679.08	3093.6	1858.9	2445.76	1.36	–	–	–

"–" denotes genes with no differences at transcriptional level, fold change ≤ 1. Some of the genes have small differences, but have a decisive impact on CA production. We also used fold change as an indicator

"No" denotes that sequence was not mapped to the genome sequence assembly of *A. niger* strain CBS 513.88

[a] Description of gene or closest homolog (BLASTP)

[b] Fold change of differentially expressed (FDR < 0.05, FPKM $\geq$ 50 in *A. niger* YX-1217 at time 10 h or time 40 h) genes based on a comparison of transcription levels at YX-1217/ATCC 1015 (designated as *S1*/*S3*) (10 h), YX-1217/YX-1217G (designated as *S1*/*S2*) (10 h), YX-1217/ATCC 1015 (designated as *S1*/*S3*) (40 h), and YX-1217/YX-1217G (designated as *S1*/*S2*) (40 h), respectively

agtC (An15g07800), and *gbeA* (An14g04190) encoding α-amylases (GH13 family), and genes *agdC* (An01g10930) and *agdA* (An04g06920) encoding α-glucosidase (family GH31) were all abundant and upregulated in YX-1217, whereas these genes were downregulated in ATCC 1015 at the two stages. However, previous reports have shown that the transcript levels of genes *glaA* (An03g06550) and *agdA* (An04g06920) in *A. niger* N402 did not significantly differ from days 2 to 8 (Jørgensen et al. 2010). In addition, the two genes displayed higher transcript levels among all genes on maltose-limited chemostat culture compared to xylose-limited chemostat culture (Jørgensen et al. 2009). GH15 possesses a starch-binding domain (SBD), which is a discrete C-terminal region that binds to starch and facilitates hydrolysis (Yuan et al. 2008). Gene 140568 (An03g06560), which encodes glucan-1,4-alpha-glucosidase with the SBD, was upregulated by fivefold in *S*1/*S*3, but the expression level of the gene was mostly unaffected in *S*1/*S*2.

In addition, genes encoding other families of enzymes, GH5, GH10, GH11, GH 12, GH26, GH27, GH28, GH47, GH61, and GH62 were significantly upregulated in *S*1/*S*3 and *S*1/*S*2, particularly 190032 (An03g00940), 11115 (An01g00780, *xynB*), and 190140 (An03g00960, *axhA)* at the two stages. However, there were exceptions; gene 90046 (An12g08280), which encodes β-fructofuranosidase, gene 30627 (An08g05230) encoding endoglucanase-4, and gene 6.376.1 (An15g04900) encoding endo-beta-1,4-glucanase D, were expressed at low levels in the three strains at the stage of 40 h. Gene An12g08280 has been also reported to be upregulated by 11-fold at day 2/day 0 and was rapidly downregulated at day 8/day 0 (Jørgensen et al. 2010), which was in agreement with our transcriptional results.

Aspergillus niger conidia possess a relatively thick-layered cell wall that is shed during germination (van Leeuwen et al. 2013). Six genes involved in chitin degradation were determined to be upregulated at the initial stage of germination in YX-1217.

In all, compared to ATCC 1015 and YX-1217G, YX-1217 showed a more powerful hydrolase system for carbohydrate utilization, which may be one of the essential reasons contributing to the rapid utilization of cornmeal starch to achieve high CA titer.

Regulation of polypeptide degradation among different *A. niger* strains

In addition to carbohydrates, cornmeal is also rich in proteins and peptides. The genome of *A. niger* encodes 198 proteases that are involved in proteolytic degradation, including nine secreted aspartyl endoproteases, ten serine carboxypeptidases, and nine dipeptidyl and tripeptidyl aminopeptidases (Pel et al. 2007). Overall, 14 peptidases were differentially expressed at the transcriptional level during CA production (Table 3), of which four aspartic peptidases, five serine carboxypeptidases, one cysteine peptidase, and one arginase were more abundant in YX-1217. These all were upregulated in *S*1/*S*3 and slightly upregulated in *S*1/*S*2 at the two stages, including gene 80863 (An14g04710, *pepA*). The transcript levels of gene 80863 has been reported to peak at day 2 and showed a sharp reduction on day 8 (Jørgensen et al. 2010), which agrees with our results. In addition, previous reports have shown that aspartyl endoproteases and carboxypeptidases are mostly active at low pH (Pel et al. 2007). Because of the acidifying properties (about pH 2.5) of *A. niger* YX-1217, four aspartic peptidases and five serine carboxypeptidases were all more abundant and upregulated in YX-1217.

Proteins and polypeptides in the medium were degraded into various amino acids by peptidases, including serine and aspartic acid, which are transported via amino acid transporters for the uptake by cells (Table 5). The significant upregulation of genes encoding the amino acid trasporters demonstrated that a greater amount of amino acids were produced in the culture of strain YX-1217 compared to YX-1217G and ATCC 1015 due to the more powerful capacity of polypeptide degradation. Obviously, the peptidase expression profile of YX-1217 during the high acid production ensured the efficient utilization of amino acids from protein hydrolysis, which may also be one of attributes of strain YX-1217 to adapt to the high production of CA.

Regulation of central metabolism of CA production among different *A. niger* strains

CA is a product of cell central metabolism, which includes various pathways such as glycolysis, TCA cycle, fatty acid metabolism, and glyoxylic acid metabolism. The observed transcriptional variations on central metabolism of CA production in *S*1/*S*3 and *S*1/*S*2 are presented in Table 4.

CA is formed mainly via cytosolic glycolysis and the subsequent mitochondrial TCA cycle. In the present study, the expression levels of genes involved in glycolysis were mostly unaffected, except for gene 9.735.1. This gene, which is predicted to be a glyceraldehyde-3-phosphate dehydrogenase (GAPDH), was upregulated nearly 11- and 25-fold in *S*1/*S*3 at the two stages. Besides its established metabolic function, GAPDH has recently been implicated in various non-metabolic processes, including transcription activation, initiation of apoptosis, and ER to Golgi vesicle shuttling, or axoplasmic transport (Tarze et al. 2007). The outstanding difference of GAPDH among strain ATCC 1015 YX-1217G and YX-1217 indicated that it should be one of the key enzymes in central

Table 3 Expression of genes involved in polypeptides degradation

Gene ID (1015)	Gene ID (513.88)	Predicted function (homolog and organism)[a]	FPKM-10 h			FPKM-40 h			Fold change[b]			
			S1	*S3*	*S2*	*S1*	*S3*	*S2*	*S1*/*S3* (10 h)	*S1*/*S2* (10 h)	*S1*/*S3* (40 h)	*S1*/*S2* (40 h)
80863	An14g04710	*pepA*, peptidase aspartic, active site	2540.17	3.11	3437.07	34,270.0	49.03	10205	9.67	–	9.44	1.74
12707	An01g00370	Peptidase aspartic, active site (AP1) (*A. phoenicis*, *apnS*)	1855.35	265.64	549.84	1602.29	42.57	742.46	2.80	1.75	5.23	1.11
5000659	An07g00950	Peptidase aspartic, active site	424.65	7.66	154.19	548.92	17.21	148.96	5.79	1.46	4.99	1.88
61129	An15g06280	peptidase aspartic, active site	210.08	26.26	37.04	605.44	97.34	112.93	3.00	2.50	2.64	2.42
11004	An09g06460	Peptidase, eukaryotic cysteine peptidase active site	388.70	1.60	484.87	200.71	31.84	42.39	7.92	−1.21	2.65	2.24
2000089	An02g04690	*cpdA*, Serine carboxypeptidases F (lysosomal cathepsin A)	182.61	5.86	423.40	2358.41	51.97	1327.78	4.96	–	5.50	–
30096	An06g00310	Peptidase S8, serine carboxypeptidases S1 (lysosomal cathepsin A)	96.75	3.44	142.95	161.62	87.04	63.09	4.81	–	–	1.36
90133	An12g05960	Peptidase S28, extracellular serine carboxypeptidase	204.37	27.80	180.01	238.87	20.48	120.63	2.88	–	3.54	
30678	An08g04490	Peptidase S28, serine peptidase	214.22	40.93	166.05	2417.0	21.60	923.24	2.39	–	6.81	1.39
30666	An08g04640	Peptidase S8 and S53, serine peptidase	107.55	3.15	166.05	349.08	6.92	220.11	5.09	–	5.65	–
1000155	An01g11340	Peptidase M24, methionine aminopeptidase MAP	87.46	3.44	145.30	72.97	3.02	28.31	4.66	–	4.59	1.37
8000249	An14g05960	Arginase family protein (*E. coli*, *speB*)	156.44	0	3.61	5.97	0.00001	0.12	∞[c]	5.43	19.18	5.60
30486	An06g01880	Peptidase M20, beta-ureidopropionase	293.47	4.54	37.29	44.86	38.18	22.38	6.01	2.98	–	1.00
40364	An11g01970	Peptidase C15, pyroglutamyl peptidase I	100.04	15.68	57.07	266.533	77.46	94.93	2.67	–	1.78	1.49
60486	An15g01980	Aminotransferase, class I and II	125.68	15.02	20.95	24.15	14.33	18.70	3.06	2.58	–	–
20000064	An04g08630	Aminotransferase, class IV	68.03	2.52	69.61	265.13	7.80	71.43	4.76	–	5.09	1.89

"–" denotes genes with no differences in transcriptional levels, fold change ≤ 1. Some of the genes have small differences, but have a decisive impact on CA production. We also used fold change as an indicator

"No" denotes that the sequence was not mapped to the genome sequence assembly of *A. niger* strain CBS 513.88

[a] Description of gene or closest homolog (BLASTP)

[b] Fold change of differentially expressed (FDR < 0.05, FPKM ≥ 50 in *A. niger* YX-1217 at time 10 or time 40) genes based on a comparison of transcription levels at YX-1217/ATCC 1015 (designated as *S1*/*S3*) (10 h), YX-1217/YX-1217G (designated as *S1*/*S2*) (10 h), YX-1217/ATCC 1015 (designated as *S1*/*S3*) (40 h), and YX-1217/YX-1217G (designated as *S1*/*S2*) (40 h), respectively

[c] The FPKM of *ATCC 1015* is zero

Table 4 Expression of genes involved in central metabolism processes

Gene ID (1015)	Gene ID (513.88)	Predicted function (homolog and organism)[a]	FPKM-10 h			FPKM-40 h			Fold change[b]			
			S1	*S3*	*S2*	*S1*	*S3*	*S2*	*S1*/*S3* (10 h)	*S1*/*S2* (10 h)	*S1*/*S3* (40 h)	*S1*/*S2* (40 h)
Glycolysis												
15000076	An13g00950	*alcB,* alcohol dehydrogenase, class V	52.65	11.95	14.25	22.79	8.00	12.23	2.13	1.88	1.51	–
50661	No	Aldehyde dehydrogenase	406.67	10.58	34.53	101.40	23.60	25.76	5.26	3.55	2.10	1.97
160032	An10g00850	Aldehyde dehydrogenase (NAD+)	154.32	1.60	6.90	7.62	3.29	8.48	6.58	4.48	1.21	–
9.735.1	No	Glyceraldehyde 3-phosphate dehydrogenase	673.82	0.32	1455.29	404.21	0.00001	421.74	11.05	−1.11	25.26	–
90161	An12g08610	*glkA*, Glucokinase	228.90	99.06	151.49	158.72	89.83	119.21	1.21	–	–	–
70571	An16g02990	Phosphoglycerate mutase	182.92	426.80	143.55	48.55	204.61	119.11	−1.22	–	−2.08	−1.29
100101	An18g01670	*pfkA*, 6-phosphofructokinase	141.71	396.31	126.75	18.73	117.42	83.83	−1.48	–	−2.65	−2.16
50068	An07g08990	*pkiA*, *pyruvate kinase*	1339.84	713.44	791.51	111.70	301.28	309.77	–	–	−1.43	−1.47
TCA cycle												
3.2152.1	An08g10920	*citB*, citrate synthase	79.42	0.07	349.09	0.34	0.16	1.10	10.06	−2.13	1.06	–
6000119	An15g01920	*mscA,* methylcitrate synthase	286.25	20.60	47.61	43.11	34.60	49.59	3.79	2.58	–	–
130482	An04g02090	*pycA*, Pyruvate carboxylase	176.18	242.37	174.54	42.81	49.14	33.15	1	1.44	–	–
20251	An02g12770	Succinate dehydrogenase SDH1	499.46	384.63	166.11	53.31	297.99	201.71	–	1.58	−2.48	−1.91
40489	An11g02550	Phosphoenolpyruvate carboxykinase (*A. nidulans*, *acuF*)	71.15	98.07	18.84	71.19	313.94	113.38	–	1.91	−2.14	–
30306	An06g00990	Fumarate reductase FRDS	199.86	270.39	99.20	38.69	307.69	145.62	–	1.01	−2.99	−1.9
50562	An07g02160	*mdh1*, malate dehydrogenase	1452.29	1178.52	1336.53	1725.86	810.04	764.45	–	–	1.09	1.17
101221	An18g06760	Isocitrate dehydrogenase, gamma subunit	1198.24	711.97	1113.35	2581.7	700.18	808.43	–	–	2.03	1.82
110571	An09g03870	Aconitase	202.23	332.86	80.18	8.67	33.42	41.12	–	–	−1.94	−2.24
40119	An11g00510	*aclB*, ATP-citrate lyase	950.20	459.53	554.44	46.72	181.23	63.03	1.05	–	−1.96	–
40123	An11g00530	*aclA*, ATP-citrate lyase	980.48	473.78	682.24	110.4	211.46	81.49	1.05	–	–	–
Fatty acid metabolism												
7000050	An16g04830	Acyl-CoA synthetase	90.11	4.06	43.06	33.90	2.32	11.33	4.47	1.06	3.86	–
170132	An04g05720	3-ketoacyl-CoA thiolase	95.82	62.70	40.55	684.04	62.88	149.85	–	1.24	3.44	2.19
13000035	An04g04330	*afeA*, acyl-CoA synthetase	196.82	0.31	113.28	10.26	1.27	2.41	9.31	–	3.01	2.81
Glyoxylic acid metabolism												
11071	An01g09270	*acuB*, isocitrate lyase	29.32	9.50	1.90	133.18	63.90	116.37	1.62	3.94	1.05	–
160030	An10g00820	*oahA*, isocitrate lyase/oxaloacetate acetylhydrolase	623.51	0.26	65.54	5.66	10.70	6.91	9.97	3.25	–	–
6000115	An15g01860	*acuE,* malate synthase	26.01	175.50	11.42	95.47	127.09	85.78	−2.75	1.18	–	–

"–" denotes genes with no differences at transcriptional level, fold change ≤ 1. Some of the genes have small differences, but have a decisive impact on CA production. We also used fold change as an indicator

"No" denotes that sequence was not mapped to the genome sequence assembly of *A. niger* strain CBS 513.88

[a] Description of gene or closest homolog (BLASTP)

[b] Fold change of differentially expressed (FDR < 0.05, FPKM ≥ 50 in *A. niger* YX-1217 at time 10 or time 40) genes based on a comparison of transcription levels at YX-1217/ATCC 1015 (designated as *S1*/*S3*) (10 h), YX-1217/YX-1217G (designated as *S1*/*S2*) (10 h), YX-1217/ATCC 1015 (designated as *S1*/*S3*) (40 h), and YX-1217/YX-1217G (designated as *S1*/*S2*) (40 h), respectively

metabolism, closely regulating the production of CA. The expression level of gene 100101 (An18g01670), which encodes 6-phosphofructokinase (6-Pfk), was downregulated in YX-1217 at the stage of 40 h. Because an increase in CA production results in feedback inhibition of 6-Pfk, a reduction in 6-Pfk activity may lead to an improvement in CA production (Ruijter et al. 1997).

CA is an important intermediate in the TCA cycle. Citrate synthase (Cs), which is a pace-making enzyme in the first step, catalyzes the condensation of oxaloacetate and acetyl-CoA to form CA, which is the most important enzyme in CA production. Two genes, namely, 6000119 (An15g01920, *mscA*) and 3.2152.1 (An08g10920, *citB*), which encode Cs, were observed at the two stages and were upregulated in *S*1/*S*3 at the stage of 10 h, whereas these were downregulated in *S*1/*S*2 at the stage of 10 h and showed no transcriptional differences at the stage of 40 h. Three genes encoding Cs in *A. niger* CBS 513.88 (An01g09940, An08g10920, and An09g06680) have been previously identified and mapped (Pel et al. 2007). *A. niger* ATCC 1015, which shares six Cs isoenzymes (202801, 48684, 126525, 176409, 35756, and 46236), including methylcitrate synthase, may contribute to the high citrate production efficiency of *A. niger* (Sun et al. 2007). However, it was previously reported that overexpression of Cs did not increase the rate of Cs production, which suggested that Cs minimally contributes to flux control in the CA biosynthetic pathway in a noncommercial strain (Ruijter et al. 2000). But, Ghulam et al. (2014) reported that CA production by overexpression of a mutant CS was significantly enhanced from 19.4 to 64.20 mg/mL. Accordingly, the Cs activity in the fermentation broth of strain YX-1217 was assessed as described (Ruijter et al. 2000), which indicated that Cs activity was higher (289U) at the stage of 10 h, whereas it decreased (83U) at the stage of 40 h. These findings coincided with the results of transcriptome analysis and indicated that, although Cs is one of the key enzymes for CA production, the upregulated expression of Cs is not a sufficient and necessary condition for the high yield of CA.

The expression of the other key enzymes in TCA cycle, such as two succinate dehydrogenases [encoded by genes 20259 (An02g12770) and 5000505 (An07g03170), respectively], malate dehydrogenase [encoded by gene 50562 (An07g02160)], isocitrate dehydrogenase [encoded by gene 101221 (An18g06760)], and aconitase [encoded by gene 110571 (An09g03870)] showed no transcriptional differences among the three strains at the two stages. Nevertheless, their expression levels as indicated by FPKM value were high during CA formation. ATP-citrate lyase is the key enzyme to catalyze the decomposition of CA to oxaloacetate (OAA) and acetyl coenzyme A, and there are two homologs in these *A. niger* strains, encoded by gene 40119 (An11g00510) and 40123 (An11g00530), respectively. Both of these enzymes maintain stable transcriptional levels and were even slightly upregulated at the stage of 10 h for strain YX-1217. These data illustrated that the TCA cycle still maintained basic activity in these *A. niger* strains, which should be an important prerequisite for these *A. niger* strains to maintain growth and survive in the living environment of high CA titers.

Glyoxylic acid cycle is the variation of TCA cycle, which forms an alternative pathway where isocitrate is converted into malate without the production of NADH by the consecutive catalysis of isocitrate lyase and malate synthase. The transcripts of two homologous encoding isocitrate lyase contain two homologous genes 11071 (An01g09270, *acuB*) and 160030 (An10g00820, *oahA*), which are highly abundant in YX-1217; however, the transcript of gene (An15g01860, *acuE*) encoding malate synthase was not obviously different in these strains.

Under the conditions of adequate oxygen, fatty acids are decomposed into acetyl-CoA and completely oxidized into CO_2 and H_2O, which consequently releases a large amount of energy. Acyl-CoA synthetase plays a major role in this process by activating long-chain fatty acids with more than 12 carbons, which encodes genes 7000050 (An16g04830) and 13000035 (An04g04330) and shows higher transcriptional level in YX-1217 than in ATCC 1015 at the two stages. The data indicated that strain YX-1217 has more powerful catabolic capacity for fatty acid than ATCC 1015, which can supply a greater amount of acetyl-CoA and energy for the growth and survival of YX-1217 to yield a greater amount of CA.

In short, the central metabolism among the three strains displayed no substantial differences, while the better central metabolism was an important premise for strain YX-1217 to overproduce CA.

Regulation of transporter mechanisms of CA production among different *A. niger* strains

Elucidating transporter mechanisms for CA production is crucial. The transcriptional variations in transporter mechanisms among the three *A. niger* strains are presented in Table 5. In this study, 25 transporters were differentially expressed at the transcriptional level, which include seven synaptic vesicle transporter SVOP and related transporters (major facilitator superfamily), four amino acid transporters, three peptide transporters, and seven ion transporters that were upregulated in YX-1217 at the two stages.

The transport functions of synaptic vesicles may be more complex than currently envisioned, which are related to eukaryotic and bacterial phosphate, sugar, and organic acid transporters (Janz et al. 1998). Seven synaptic vesicle trafficking proteins were upregulated in *S*1/*S*3

Table 5 Expression of genes involved in transporter mechanisms

Gene ID (1015)	Gene ID (513.88)	Predicted function (homolog and organism)[a]	FPKM-10 h			FPKM-40 h			Fold change[b]			
			S1	*S3*	*S2*	*S1*	*S3*	*S2*	*S1*/*S3* (10 h)	*S1*/*S2* (10 h)	*S1*/*S3* (40 h)	*S1*/*S2* (40 h)
2.412.1	An02g08970	Synaptic vesicle transporter SVOP and related transporters (major facilitator superfamily)	185.2	2.21	94.74	21.26	4.17	5.31	6.38	–	2.44	2.00
3000074	An08g10970	Synaptic vesicle transporter SVOP and related transporters	160.28	0.71	917.73	6.31	9.60	11.21	7.80	− 2.51	–	–
160123	An17g01710	Synaptic vesicle transporter SVOP and related transporters	103.76	2.77	49.29	930.44	2.51	122.66	5.22	1.07	8.53	2.92
5000334	An07g05880	Synaptic vesicle transporter SVOP and related transporters	107.56	4.57	49.04	70.54	8.35	23.06	4.55	1.13	3.07	1.61
5.1708.1	No	Synaptic vesicle transporter SVOP and related transporters	24.18	2.10	58.59	323.21	43.80	63.16	3.52	− 1.27	2.88	2.35
160129	An10g00690	Permease of the major facilitator superfamily	118.95	0.44	26.12	13.04	6.55	0.91	8.07	2.18	–	3.83
9000464	An12g03550	Permease of the major facilitator superfamily	80.14	1.01	28.94	53.88	13.55	1.50	6.29	1.46	1.99	5.16
31842	An08g03200	Ammonia permease	658.74	11.45	452.98	874.63	583.09	67.70	5.84	–	–	3.69
8.781.1	An14g02390	Ammonia permease	95.62	5.25	9.21	6.99	7.80	5.15	4.18	3.37	–	–
150043	No	Amino acid transporters	313.46	3.98	494.76	1872.15	1170.98	219.82	6.30	–	–	3.09
18.284.1	An16g07900	Amino acid transporters	91.62	2.61	2.59	60.14	8.98	12.63	5.13	5.14	2.74	2.25
11.172.1	An09g02550	Amino acid transporters	85.21	1.01	3.44	178.80	4.02	13.43	6.39	4.63	5.47	3.73
19000022	An03g01590	Amino acid transporters	77.90	0.49	6.71	79.07	7.25	1.22	7.32	3.53	3.44	6.01
51440	An07g01950	Xanthine/uracil transporters (*A. nidulans, uapC*)	103.74	21.22	60.84	245.16	194.55	16.35	2.28	–	–	3.90
31302	An08g06240	Uridine permease/thiamine transporter/allantoin transport	60.46	4.80	28.19	269.89	72.22	3.70	3.65	1.10	1.90	6.18
110148	No	Tetrapeptide transporter, OPT1/isp4	1213.89	6.69	1523.02	1328.97	230.62	666.57	6.18	–	2.52	–
18.109.1	An16g06770	Monocarboxylate transporter	45.49	6.18	11.67	106.08	12.00	24.68	2.87	1.95	3.14	2.10
111102	An09g00660	Oligopeptide transporter OPT superfamily	20.89	0.33	96.18	570.88	25.23	123.98	6.00	− 2.20	4.49	2.20
21.45.1	An12g10320	Fe^{2+}/Zn^{2+} regulated transporter	111.77	5.31	126.14	2585.52	606.42	499.30	4.39	–	2.09	2.37
10845	An01g03790	Na+: solute symporter	74.05	3.14	53.95	51.89	51.48	2.18	4.56	–	–	4.57
1001002	An01g01950	Mg^{2+} transporter protein, CorA-like	42.43	0.98	12.76	461.93	187.17	408.91	5.44	1.73	1.30	–
9000143	An12g07730	Ctr Cu^{2+} transporter	79.63	16.88	94.62	518.01	27.41	58.48	2.23	–	4.24	3.14
22.68.1	An04g09850	*git1*, Inorganic phosphate transporter	16.87	1.25	20.28	100.07	22.88	14.74	3.75	–	2.12	2.76
240077	An19g00340	Ca2+/H+ antiporter VCX1 and related proteins	50.22	0.86	15.81	615.05	81.96	175.32	5.77	1.58	2.98	1.89
240035	An19g00330	Ca2+/H+ antiporter VCX1 and related proteins	29.77	2.50	15.81	204.99	28.69	92.59	3.57	–	2.83	1.15

"–" denotes genes with no differences at transcriptional level, fold change ≤ 1. Some of the genes have small differences, but have a decisive impact on CA production. We also used fold change as an indicator

"No" denotes that sequence was not mapped to the genome sequence assembly of *A. niger* strain CBS 513.88

[a] Description of gene or closest homolog (BLASTP)

[b] Fold change of differentially expressed (FDR < 0.05, FPKM ≥ 50 in *A. niger* YX-1217 at time 10 or time 40) genes based on a comparison of transcription levels at YX-1217/ATCC 1015 (designated as *S1*/*S3*) (10 h), YX-1217/YX-1217G (designated as *S1*/*S2*) (10 h), YX-1217/ATCC 1015 (designated as *S1*/*S3*) (40 h), and YX-1217/YX-1217G (designated as *S1*/*S2*) (40 h), respectively

and *S*1/*S*2. In strain YX-1217, abundant synaptic vesicles could accelerate the absorption and utilization of materials such as sugar that were prepared for the production of CA. In addition, synaptic vesicle trafficking associated with neuronal development, macromolecules, small molecules, and ion transport is regulated by a voltage-dependent Ca^{2+} channel (Augustine et al. 1987; Zhang et al. 2013). Vesicle initiation and subsequent membrane fusion both require an increase in Ca^{2+} concentration in the cytoplasm. The cytosolic Ca^{2+} levels are determined by two opposite fluxes, namely, Ca^{2+} influx via channels and Ca^{2+} efflux via active transporters (Waditee et al. 2004). Furthermore, changes in intracellular Ca^{2+} distribution affect ion homeostasis. Genes involved in various ion transport proteins for Na^{+}, K^{+}, Fe^{2+}, Ca^{2+}, Mg^{2+}, Zn^{2+}, and Cu^{2+} were differentially expressed in the three strains. Two important genes, namely, 240077 (An19g00340) and 240035 (An19g00330), which encode a Ca^{2+}/H^{+} antiporter of Vcx1 and related proteins, showed significantly higher transcriptional levels in *S*1/*S*3, whereas these were slightly upregulated in *S*1/*S*2. The results showed that these genes were associated with maintaining a low cytosolic-free Ca^{2+} concentrations by catalyzing pH gradient-energized vacuolar Ca^{2+} accumulation in *A. oryzae RIB40.*

The transcription levels of four amino acid transporters were elevated in the three strains. Gene 18.284.1 (An16g07900) is similar to a choline transporter Hnm1 in *A. fumigatus* Af293, which is associated with nitrogen uptake. Gene 11.172.1 (An09g02550) is similar to a putative GABA permease GabA, which was upregulated in *S*1/*S*3 and *S*1/*S*2 at the two stages. Genes involved in other small molecule transport (ammonium, xanthine, uracil, thiamine, urea, and peptides) exhibited high levels of mRNA expression in the three strains (Table 5).

The significant upregulation of the transporters showed the more powerful transporter capacity of materials in strain YX-1217 compared to YX-1217G and ATCC1015, which enables YX-1217 to quickly and sufficiently transport substances (macromolecules, small molecules, and ions) into, out of, or within a cell. It may also be one of the attributes of strain YX-1217 to adapt to the high production of CA.

Regulation of energy metabolism, transcription factor regulation, and resistance among different *A. niger* strains

The maintenance of energy balance is critical for high CA fermentation. Increased transcript levels were detected in YX-1217 such as genes 21.34.1 (An12g09940), 9.1179.1 (An05g00300), and 40169 (An11g04370) encoding cytochrome 5; gene 3.1942.1 (An08g06550) encoding ubiquinol cytochrome c reductase; and gene 4.1469.1 encoding cytochrome c heme-binding proteins (Table 6). Most of their FPKM values were highly expressed in the three strains at the two stages, and mRNA expression was upregulated at the stage of 40 h compared to 10 h. This result showed that a large amount of energy was produced by the respiratory chain to maintain the energy balance and supply energy for CA production during the high CA production period in YX-1217. Novodvorska et al. (2013) detected increased transcript levels for genes encoding putative subunits of the respiratory chain mainly during the first hour of germination such as cytochrome b (An11g04370), which would supply energy for spore germination. Moreover, the present study detected important genes such as 2000458 (An02g06550), 5000079 (An07g08760), 6000073 (An15g00690), and 2.1052.1 (An02g09730), encoding relatives of NADH/NADPH oxidase, which catalyze the regeneration of $NAD^{+}/NADP^{+}$. These genes were upregulated in YX-1217 at the stage of 40 h. To maintain the balance of intracellular redox state and energy metabolism, the superfluous reducing power NADH must be converted to its oxidation state NAD^{+} in time by a regeneration system for $NAD^{+}/NADP^{+}$, otherwise the metabolism of glucose to CA will be arrested. In a successful CA-producing strain, a powerful regeneration system for $NAD^{+}/NADP^{+}$ is needed to convert the mass production of NADH/NADPH along with the CA overproduction.

Genes encoding proteins that are involved in transcription and translation were upregulated in YX-1217. Gene 800003 (An18g04840), encoding translational elongation factor EF-1 alpha, was upregulated by at least 26-fold. It was associated with the binding reaction of aminoacyl-tRNA (AA-tRNA) to ribosomes, which laid a good foundation for rapid synthesis of a series of enzymes involved in CA production. Genes of transcription factors involved in pH regulation in YX-1217 are presented in Table 6. Gene 2000159 (An02g07890) is the pH-responsive regulator PacC of *Aspergillus*, which has been implicated in the regulation of genes encoding transporter proteins such as GABA (*γ*-amino *n*-butyrate) permease and phosphate permease (Peñalva et al. 2002). CA production in *A. niger* begins at pH 3.0 and is optimal just below pH 2.0 (Haq et al. 2005). Some reports on the sensitivity of hypoxia in filamentous fungi to intracellular pH refer to the reduced activity of plasma membrane H+ ATPase, which is involved in the maintenance of intracellular proton concentrations by extrusion of protons from the cytoplasm at the expense of ATP (Andersen et al. 2009). Therefore, acid concentration affects the internal pH of cells.

Fungi rely on resistance to scavenge reactive oxygen species (ROS) that can cause cell damage by oxidizing cell components such as DNA, proteins, and lipids and can also compromise cell functions (Devasagayam et al.

Table 6 Expression of genes involved in energy metabolism, transcription factor regulation, and resistance mechanism

Gene ID (1015)	Gene ID (513.88)	Predicted function (homolog and organism)[a]	FPKM-10 h			FPKM-40 h			Fold change[b]			
			S1	*S3*	*S2*	*S1*	*S3*	*S2*	*S1*/*S3* (10 h)	*S1*/*S2* (10 h)	*S1*/*S3* (40 h)	*S1*/*S2* (40 h)
Energy metabolism												
9.1179.1	An05g00300	Cytochrome b5 (*Musca domestica, cytb5*)	43.10	208.68	41.02	1503.85	162.33	333.18	−2.27	–	3.21	2.17
40169	An11g04370	Cytochrome b5	1411.35	658.03	895.69	5202.49	565.65	883.43	1.10	–	3.20	2.55
21.34.1	An12g09940	Cytochrome b5	69.63	3.12	4.94	1.49	0.33		4.47	3.81	2.17	–
3.1942.1	An08g06550	Ubiquinol cytochrome c reductase, subunit QCR8	944.78	1718.06	1690.58	6710.39	755.36	1955.17	–	–	3.15	1.77
4.1469.1	No	Cytochrome c heme-binding site	34.15	9.48	30.55	185.57	28.69	80.69	1.84	–	2.69	1.20
2000458	An02g06550	Ferric reductase, NADH/NADPH oxidase and related proteins	109.62	6.85	5.55	4.73	4.43	2.40	3.99	4.30	–	–
6000073	An15g00690	NADH:ubiquinone oxidoreductase, NDUFA6/B14 subunit	336.69	335.46	351.26	1782.8	206.93	367.27	–	–	3.10	2.27
2.1052.1	An02g09730	NADH:ubiquinone oxidoreductase, NDUFB7/B18 subunit	588.21	870.88	791.99	3764.33	578.95	671.06	–	–	2.70	2.49
Transcription factor												
1.2786.1	An01g13950	Upstream transcription factor 2/L-myc-2 protein	92.02	0	21.14	543.05	39.25	183.80	∞[c]	2.12	3.79	1.56
80804	An14g04200	*rghB*, transcription initiation factor TFIID, subunit BDF1 and related bromodomain proteins, rhamnogalacturonase B	101.42	3.72	19.40	46.80	6.79	2.75	4.76	2.38	2.78	
5.1343.1	An07g07370	Transcription factor, Myb superfamily	46.57	4.25	31.47	134.79	71.56	1.04	3.45	–	–	–
8.1025.1	An14g00780	Putative translation initiation inhibitor UK114/IBM1	98.99	26.99	80.59	1084.41	129.09	105.30	1.87	–	3.07	3.36
800003	An18g04840	Translation elongation factor EF-1 alpha/Tu	630.05	1919.49	2031.67	1059.85	0.00001	0.00001	-1.60	-1.68	26.65	26.65
12000021	An12g00240	Putative translation initiation inhibitor UK114/IBM1	664.05	638.32	624.75	2105.6	187.81	208.68	–	–	3.48	2.04
1000929	An01g02900	Translation initiation factor 5A (*S. cerevisiae, anbA*)	1299.2	2868.77	1426.52	3715.03	808.85	1219.28	–	–	2.19	1.61
2000159	An02g07890	*pacC*, pH-response transcription factor	91.52	55.30	39.50	29.38	89.03	32.46	–	1.21	−1.60	–
Resistance mechanism												
20494	An02g02750	Catalase	59.61	35.89	8.12	68.79	9.45	19.16	–	2.87	2.86	1.84
10568	An01g01550	Catalase (*A. fumigates, cat1*)	257.06	106.96	4.78	0.33	56.87	5.29	1.26	5.74	−7.42	−3.99
1.973.1	An01g12530	Manganese superoxide dismutase	1308.37	30.85	3758.22	116.36	9.46	1.82	5.40	−1.52	3.62	5.97
10.1058.1	An18g00260	Cytochrome P450 CYP3/CYP5/CYP6/CYP9 subfamilies (*A. parasiticus, avnA*)	69.73	2.98	75.30	126.19	9.63	20.70	4.54	–	3.71	2.60

Table 6 continued

Gene ID (1015)	Gene ID (513.88)	Predicted function (homolog and organism)[a]	FPKM-10 h			FPKM-40 h			Fold change[b]			
			S1	*S3*	*S2*	*S1*	*S3*	*S2*	*S1*/*S3* (10 h)	*S1*/*S2* (10 h)	*S1*/*S3* (40 h)	*S1*/*S2* (40 h)
11000284	An09g03210	Cytochrome P450 CYP2 subfamily	92.33	21.67	17.98	175.49	3.08	22.36	2.09	2.36	5.83	2.97
130837	An04g00480	Basic-leucine zipper (bZIP) transcription factor	119.36	42.05	114.03	223.53	644.36	74.15	1.50	–	− 1.53	1.59
4000214	An11g05340	FAD-dependent oxidoreductase	534.85	43.75	408.23	37.98	20.96	39.89	3.61	–	–	–
160248	An17g00010	Copper amine oxidase (*H. polymorpha AMO*)	2319.99	1.33	4.91	4.92	2.37	2.71	10.77	8.88	1.05	–
150032	An13g00710	Copper amine oxidase AO-1	944.56	7.30	16.52	133.7	37.95	78.39	7.30	5.83	1.81	–
110401	An09g01550	*ao-1*, copper amine oxidase	713.37	0.95	9.10	222.50	23.89	22.92	9.55	6.29	3.21	3.27
19000158	An03g00730	Hypothetical copper amine oxidase with signal peptide motif	255.57	13.09	25.24	116.39	32.08	36.72	4.28	3.34	1.85	1.66
50349	An07g08720	Glycosyl transferase, family 20, trehalose-6-phosphate synthase	115.01	19.63	14.41	11.60	69.86	71.36	2.55	2.99	− 2.58	− 2.62
80430	An14g02180	*tpsB*, trehalose-6-phosphate synthase component TPS1 and related subunits	41.24	23.10	6.07	7.16	24.02	19.63	–	2.76	− 1.74	− 1.45

"–" denotes genes with no differences at transcriptional level, fold change ≤ 1. Some of the genes have small differences, but have a decisive impact on CA production. We also used fold change as an indicator

"No" denotes that sequence was not mapped to the genome sequence assembly of *A. niger* strain CBS 513.88

[a] Description of gene or closest homolog (BLASTP)

[b] Fold change of differentially expressed (FDR < 0.05, FPKM $\geq$ 50 in *A. niger* YX-1217 at time 10 or time 40) genes based on a comparison of transcription levels at YX-1217/ATCC 1015 (designated as *S1*/*S3*) (10 h), YX-1217/YX-1217G (designated as *S1*/*S2*) (10 h), YX-1217/ATCC 1015 (designated as *S1*/*S3*) (40 h), and YX-1217/YX-1217G (designated as *S1*/*S2*) (40 h), respectively

[c] The FPKM of *ATCC 1015* is zero

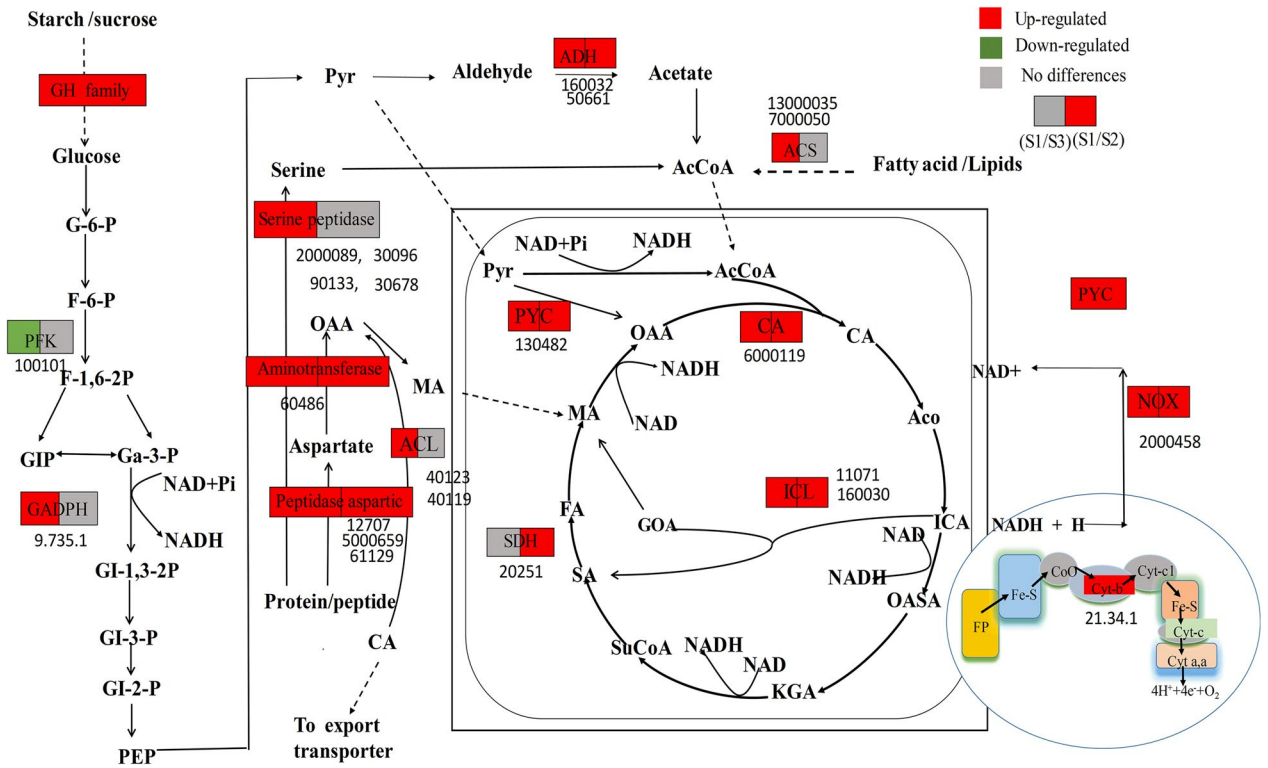

Fig. 5 Transcription level regulation of genes involving CA production in three different *A. niger* at 10 h. Upregulated, downregulated, and no differentially expressed genes involving CA production are highlighted in red, green, and gray color, respectively. Comparative transcriptomic differences of strain YX-1217 versus ATCC 1015 (*S1*/*S3*) and strain YX-1217 versus YX-1217G (*S1*/*S2*) at 10 h are exhibited, respectively, in squares. *PFK* 6-phosphofructokinase, *GADPH* glyceraldehyde-3-phosphate dehydrogenase, *PYC* pyruvate carboxylase, *ACS* acetyl-coA synthetase, *ADH* alcohol dehydrogenase, *CS* citrate synthase, *ICL* isocitrate lyase, *SDH* succinate dehydrogenase, *ACL* ATP-citrate lyase, *NOX* NADH/NADPH oxidase

2004; Kroneck and Torres 2015; Fountain et al. 2016). Catalase, superoxidase, and oxidoreductases can protect cells by opposing oxidative stress during growth and development. The transcript levels of these genes that are involved in resistance were relatively high in the three strains and were significantly upregulated in YX-1217 at the two stages. Gene 1.973.1 (An01g12530), involved in manganese and iron superoxide dismutase, showed higher expression in *S1*/*S3* at the stage of 10 h, as well as in *S1*/*S3* and *S1*/*S2* at the stage of 40 h. Antioxidant defense systems to scavenge ROS can decrease cell damage and retard cell aging. A previous report has indicated that the knockout of five catalase family genes (*catA*, *catB*, *catC*, *catD*, and *catP*) can lead to a significant decrease in anti-oxidative capability, UV-B resistance, and virulence in *B. bassiana* (Wang et al. 2013). The overexpression of a cytosolic manganese-cored SOD (Bbsod2) in *B. bassiana* leads to significantly enhanced anti-oxidative capability and UV-B resistance. Knocking out three superoxide dismutase genes (*sod1*, *sod4*, and *sod5*) in *B. bassiana* could lead to significant decreases in anti-oxidative capability (Xie et al. 2010a, b). The expression of bZIP transcription factors such as *atf21* and *atfA* has been shown to regulate aflatoxin production in response to oxidative stress in vitro during early stages of fungal growth (Fountain et al. 2016). The overexpression of five bZip transcription factors (RsmA, Napa, ZipA, ZipB, and ZipC) in *A. nidulans* results in the significant improvement of resistance to ROS (Yin et al. 2013). To obtain a CA production strain with a higher yield, it is essential to investigate genes that are involved in resistance mechanism.

Taken together, the findings of the present study indicate that a highly efficient electron transport chain, a regeneration system for NAD^+/$NADP^+$, the highly upregulated expression of key genes involved in transcription and translation protein, and an effective resistance mechanism apparently contribute to high CA production in *A. niger* YX-1217.

Transcription regulation of genes involving CA production among three different *A. niger* strains

To elucidate the mechanism underlying CA yield, the central metabolic pathways were first assessed in terms of their direct correlation to CA production (Figs. 5 and 6).

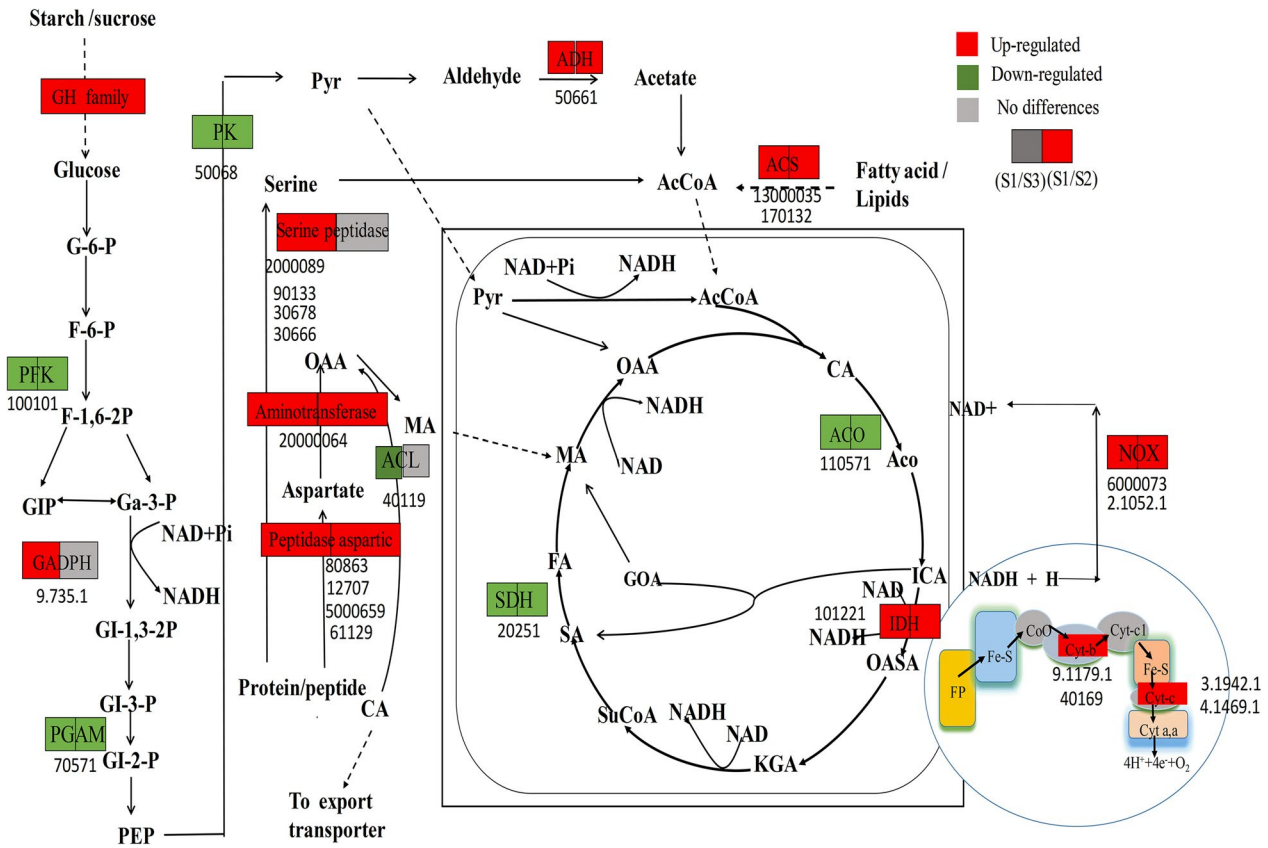

Fig. 6 Transcription level regulation of genes involving CA production in three different *A. niger* at 40 h. Upregulated, downregulated, and no differentially expressed genes involving CA production are highlighted in red, green, and gray, respectively. Comparative transcriptomic differences of strain YX-1217 versus ATCC 1015 (*S1*/*S3*) and strain YX-1217 versus YX-1217G (*S1*/*S2*) at 40 h are exhibited, respectively, in squares. *PFK* 6-phosphofructokinase, *GADPH* glyceraldehyde-3-phosphate dehydrogenase, *PGAM* phosphoglycerate mutase, *PK* pyruvate kinase, *ACS* acetyl-coA synthetase, *ADH* alcohol dehydrogenase, *ACO* aconitase, *IDH* isocitrate dehydrogenase, *SDH* succinate dehydrogenase, *ACL* ATP-citrate lyase, *NOX* NADH/NADPH oxidase

The results indicate that the transcriptional levels of most of the key genes contributing to CA yield are significantly higher in *A. niger* YX-1217 than in strain YX-1217G and ATCC 1015 during conidia germination. The genes encoding the GH family for carbohydrate hydrolysis and the genes encoding proteins/peptides degeneration were upregulated in *A. niger* YX-1217 during conidial germination. It should be related to its powerful capacity to utilize cornmeal fluidified liquid as raw material for the production of CA.

Gene 9.735.1, encoding GAPDH that catalyzes the conversion of glyceraldehyde 3-phosphate to D-glycerate 1,3-bisphosphate, was upregulated by nearly 11- and 25-fold in *S1*/*S3*, whereas there was no differential expression in *S1*/*S2*. In TCA metabolism, the significantly upregulated expression of some key genes such as 6000119 (An15g01920) and 3.2152.1 (An08g10920), which encode Cs, a crucial enzyme in CA production that catalyzes the condensation reaction of acetyl coenzyme A and oxaloacetate to form CA, was upregulated in *S1*/*S3*. In terms of lipid metabolism, the transcript of genes 7000050 (An16g04830) and 13000035 (An04g04330), which encode Acyl-CoA synthetase that convert fatty acid molecules into acyl-coenzyme A for their subsequent oxidation, was highly abundant in *S1*/*S3* at the two stages. Furthermore, some important genes, 2000458 (An02g06550), 5000079 (An07g08760), 6000073 (An15g00690), and 2.1052.1 (An02g09730) that encode relatives of NADH/NADPH oxidase catalyze the regeneration of NAD^+/$NADP^+$. In the present study, these genes were upregulated in YX-1217.

Interestingly, some genes associated with CA production have no obvious differences or have low transcriptional expression in the three strains at the stage of 40 h. Filamentous fungi utilize a feedback mechanism termed repression under secretion stress (RESS), which selectively downregulates the transcription of genes encoding extracellular enzymes upon ER stress and thus helps

Table 7 Gene expression verification by qRT-PCR

Gene ID	Predicted function (homolog and organism)	RNA-Seq				qRT-PCR			
		S1/S3 (10 h)	*S1/S2* (10 h)	*S1/S3* (40 h)	*S1/S2* (40 h)	*S1/S3* (10 h)	*S1/S2* (10 h)	*S1/S3* (40 h)	*S1/S2* (40 h)
190032	GH 10, endo-1,4-beta-xylanase F1	11.24	9.96	6.05	2.58	10.69	8.42	5.50	1.93
80523	*eglA*, GH 12, endoglucanase A	7.9	5.43	4.3	−2.12	6.3	4.21	4.1	−1.1
190140	*axhA*, GH 62, alpha-L-arabinofuranosidase	8.36	7.59	8.47	3.08	7.41	6.38	6.54	2.01
6000119	*mscA*, methylcitrate synthase	3.79	2.58	0.31	0.20	3.45	2.45	0.20	0.10
12707	Peptidase aspartic, active site (AP1) (*A. phoenicis, apnS*)	2.80	1.75	5.23	1.11	2.11	1.54	4.37	1.00
7000050	Acyl-CoA synthetase	4.47	1.06	3.86	0.45	3.98	1.01	3.55	0.22
160123	Synaptic vesicle transporter SVOP and related transporters	5.22	1.07	8.53	2.92	6.45	0.67	9.36	2.44
11.172.1	Amino acid transporters	6.39	4.63	5.47	3.73	7.65	5.00	6.57	2.84

All data were ratio log2

Genes based on a comparison of transcription levels at YX-1217/ATCC 1015 (designated as *S1/S3*) (10 h), YX-1217/YX-1217G (designated as *S1/S2*) (10 h), YX-1217/ATCC 1015 (designated as *S1/S3*) (40 h), and YX-1217/YX-1217G (designated as *S1/S2*) (40 h), respectively

to reduce the ER load (Fan et al. 2015). RESS represses the transcription of secretory protein genes under ER stress conditions in *T. reesei*, *A. niger*, and *A. nidulans* (Wang et al. 2010). In *A. niger*, RESS leads to the selective transcriptional downregulation of the glucoamylase gene (Alsheikh et al. 2004). Transcriptome profiling of *N. crassa* has revealed that the expression of most lignocellulase genes are significantly induced at early time points (16 h), but rapidly declines thereafter, implying that RESS exists in *N. crassa* and might be a limiting step of lignocellulase synthesis (Wang et al. 2010), which agrees with our findings. At the peak time of the CA production, RESS could result in the downregulation of the key genes involved in CA production.

Experimental validation of gene expression level by qRT-PCR

To verify the expression level of the genes identified by RNA-Seq, eight genes highly related to the CA production were selected and qRT-PCR was performed. The majority of these candidates exhibited upregulated expression in *S1/S3* and *S1/S2* at the stage of 10 h, and only a minority of genes exhibited downregulated expression in *S1/S3* and *S1/S2* at the stage of 40 h (Table 7). The results coincide with the findings of RNA-Seq and qRT-PCR analyses, thus indicating that our results were effective and reliable.

Conclusions

In this study, to explore the metabolic mechanism and physiological phenotype associated with high CA productivity, the transcriptomes of high CA-producing *A. niger* YX-1217 and degenerative YX-1217G were investigated and compared using *A. niger* ATCC1015 as a control. The results revealed the striking transcriptional differences in CA production among the three *A. niger* strains. In the carbohydrate hydrolysis and polypeptide degradation pathway, many key genes were upregulated in YX-1217, which showed a more powerful hydrolase system for carbohydrate utilization. It may be one of the essential reasons contributing to the rapidly utilization of cornmeal starch to achieve high CA titer. In central metabolism, the three strains displayed no substantial differences, while the better central metabolism was an important premise for strain YX-1217 to overproduce CA. A total of 25 protein transporters were differentially expressed in YX-1217, which could accelerate the absorption and utilization of materials such as sugar that were prepared for the production of CA. In addition, a relatively strong electron transport chain, a regeneration system for $NAD^+/NADP^+$, and an efficient resistance mechanism may have contributed to the high CA production rate of *A. niger* YX-1217. These results will undoubtedly help us to comprehensively understand the character of *A. niger* and pave the way for further research on fungi.

Additional files

Additional file 1: Table S1. The appendix file linking the CBS 513.88 annotation to ATCC 1015 annotation.

Additional file 2: Table S2. Primers used in qRT-PCR analysis.

Additional file 3: Table S3. Number of clean reads and mapping ratio in three *A. niger* strains.

Additional file 4: Table S4. Details of the upregulated genes and all FPKM values in S1/S3 at h.

Additional file 5: Table S5. Details of the downregulated genes and all FPKM values in S1/S3 at 10 h.

Additional file 6: Table S6. Details of the upregulated genes and all FPKM values in S1/S3 at 40 h.

Additional file 7: Table S7. Details of the downregulated genes and all FPKM values in S1/S3 at 40 h.

Additional file 8: Table S8. Details of the upregulated genes and all FPKM values in S1/S2 at 10 h.

Additional file 9: Table S9. Details of the downregulated genes and all FPKM values in S1/S2 at 10 h.

Additional file 10: Table S10. Details of the upregulated genes and all FPKM values in S1/S2 at 40 h.

Additional file 11: Table S11. Details of the upregulated genes and all FPKM values in S1/S2 at 40 h.

Abbreviations

A. niger: *Aspergillus niger*; *A. nidulans*: *Aspergillus nidulans*; *T. reesei*: *Trichoderma reesei*; CA: citric acid; OA: oxalic acid; FPKM: fragments per kilobase of exon model per million mapped reads; FDR: false discovery rate; KEGG: The Kyoto Encyclopedia of Genes and Genomes database; qRT-PCR: real-time quantitative RT-PCR; S1: *A. niger* YX-1217; S2: *A. niger* YX-1217G; S3: ATCC 1015; SBD: starch-binding domain; OAA: oxaloacetate; AcCoA: acetyl coenzyme A; GH: glycoside hydrolase; PFK: 6-phosphofructokinase; GADPH: glyceraldehyde-3-phosphate dehydrogenase; PYC: pyruvate carboxylase; PGAM: phosphoglycerate mutase; PK: pyruvate kinase; ACS: acetyl-coA synthetase; ADH: alcohol dehydrogenase; ACO: aconitase; IDH: isocitrate dehydrogenase; CS: citrate synthase; ICL: isocitrate lyase; SDH: succinate dehydrogenase; ACL: ATP-citrate lyase; NOX: NADH/NADPH; RESS: oxidase repression under secretion stress.

Authors' contributions

HX and FQW designed the experiments. QYM supplied *A. niger* YX-1217 and YX-1217G. HX performed the experiments and analyzed the data. FQW and DZW provided reagents and materials. HX wrote the manuscript. FQW revised the manuscript. All authors read and approved the final manuscript.

Author details

[1] State Key Lab of Bioreactor Engineering, Newworld Institute of Biotechnology, East China University of Science and Technology, Shanghai 200237, China. [2] Weifang Ensign Industry Co., Ltd., Weifang 262499, China. [3] Life Science College, Henan Agricultural University, Zhengzhou 450002, China.

Acknowledgements

The authors thank the Shan Dong Weifang Ensign Industry Co., Ltd. (Weifang, China) for donating the industrial strains of *A. niger* YX-1217 and *A. niger* YX-1217G.

Competing interests

The authors declare that they have no competing interests.

Availability of data and materials

All data generated and analyzed during this study were included in the manuscript in the form of graphs and tables. The authors will provide any missing data on request.

Consent for publication

Not applicable.

Ethics approval and consent to participate

Not applicable.

Funding

The National Special Fund for State Key Laboratory of Bioreactor Engineering supported this study.

Publisher's Note

Received: 5 January 2018 Accepted: 8 May 2018
Published online: 15 May 2018

References

Adav SS, Li AA, Manavalan A, Punt P, Sze SK (2010) Quantitative iTRAQ secretome analysis of *Aspergillus niger* reveals novel hydrolytic enzymes. J Proteome Res 9:3932–3940

Alsheikh H, Watson AJ, Lacey GA, Punt PJ, MacKenzie DJ, Jeenes DJ, Pakula T, Penttilä M, Alcocer MJC, Archer DB (2004) Endoplasmic reticulum stress leads to the selective transcriptional downregulation of the glucoamylase gene in *Aspergillus niger*. Mol Microbiol 53:1731–1742

Andersen MR, Nielsen ML, J Nielsen (2008) Metabolic model integration of the bibliome, genome, metabolome and reactome of *Aspergillus niger*. Mol Syst Biol 4:178

Andersen MR, Lehmann L, Nielsen J (2009) Systemic analysis of the response of *Aspergillus niger* to ambient pH. Genome Biol 10:R47

Andersen MR, Salazar MP, Schaap PJ et al (2011) Comparative genomics of citric-acid-producing *Aspergillus niger ATCC 1015* versus enzyme-producing CBS 513.88. Genome Res 21:885–897

Augustine GJ, Charlton MP, Smith SJ (1987) Calcium action in synaptic transmitter release. Annu Rev Neurosci 10:633–693

de Oliveira JM, van Passel MW, Schaap PJ, de Graaff LH (2011) Proteomic analysis of the secretory response of *Aspergillus niger* to D-maltose and D-xylose. PLoS ONE 6:e20865

Devasagayam T, Tilak JC, Boloor KK, Sane KS, Ghaskadbi SS, Lele RD (2004) Free radicals and antioxidants in human health: current status and future prospects. JAPI 52:794–804

Fan FY, Ma GL, Li JG, Liu Q, Benz JP, Tian CG, Ma YH (2015) Genome-wide analysis of the endoplasmic reticulum stress response during lignocellulase production in *Neurospora crassa*. Biotechnol Biofuels 8:1–17

Fountain JC, Bajaj P, Pandey M, Nayak SN, Yang L, Kumar V, Jayale AS, Citikineni A, Zhang W, Scully BT, Lee RD, Kemerait RC, Varshney RK, Guo B (2016) Oxidative stress and carbon metabolism influence aspergillus flavus transcriptome composition and secondary metabolite production. Sci Rep 6:38747

Ghulam M, Aisha T, Muhammad A, Mehboob-Ur R, Amer J (2014) Comparative sequence analysis of citrate synthase and 18s ribosomal DNA from a wild and mutant strains of *Aspergillus niger* with various fungi. Bioinformation 10:1–7

Haq I-UL, Ali S, Qadeer MA (2005) Influence of dissolved oxygen concentration on intracellular pH for regulation of Aspergillus niger growth rate during citric acid fermentation in a stirred tank bioreactor. Int J Biol Sci 1(1):34–41

Janz R, Hofmann K, Südhof TC (1998) Svop, an evolutionarily conserved synaptic vesicle protein, suggests novel transport functions of synaptic vesicles. J Neurosci 18:9269–9281

Jørgensen TR, Goosen T, van den Hondel C, Lversen JJL (2009) Transcriptomic comparison of *Aspergillus niger* growing on two different sugars reveals coordinated regulation of the secretory pathway. BMC Genomics 10:44

Jørgensen TR, Nitsche BM, Lamers GE, Arentshorst M, Ca VDH, Ram AF (2010) Transcriptomic insights into the physiology of *Aspergillus niger* approaching a specific growth rate of zero. Appl Environ Microbiol 76:5344–5355

Krijgsheld P, Bleichrodt R, vanVeluw GJ, Wang F, Müller WH, Dijksterhuis J, Wösten HAB (2013) Development in *Aspergillus*. Stud Mycol 74:1–29

Kroneck PMH, Torres MES (2015) Sustaining life on planet earth: metalloenzymes mastering dioxygen and other chewy gases. Metal ions in life sciences, vol 15, pp 1–12
Nitsche BM, Jørgensen TR, Akeroyd M, Meyer V, Ram AFJ (2012) The carbon starvation response of *Aspergillus niger* during submerged cultivation. BMC Genomics 13:318
Novodvorska M, Hayer K, Pullan ST, Wilson R, Blythe MJ, Stam H, Stratford M, Archer DB (2013) Trancriptional landscape of *Aspergillus niger* at breaking of conidial dormancy revealed by RNA-sequencing. BMC Genomics 14:1–18
Pel HJ, de Winde JH, Archer DB et al (2007) Genome sequencing and analysis of the versatile cell factory *Aspergillus niger CBS 513.88*. Nat Biotechnol 25:221–231
Peñalva MA, Arst HN Jr (2002) Regulation of gene expression by ambient pH in filamentous fungi and yeasts. Microbiol Mol Biol Rev 66:426–446
Ruijter GJ, Panneman H, Visser J (1997) Overexpression of phosphofructokinase and pyruvate kinase in citric acid-producing *Aspergillus niger*. Biochem Biophys Acta 1334:317–326
Ruijter GJG, Panneman H, Xu DB, Visser J (2000) Properties of *Aspergillus niger* citrate synthase and effects of cita overexpression on citric acid production. FEMS Microbiol Lett 184:35–40
Steiger MG, Mach RL, Mach-Aigner AR (2009) An accurate normalization strategy for RT-qPCR in *Hypocrea jecorina* (*Trichoderma reesei*). J Biotechnol 145:30–37
Sun JB, Lu X, Rinas U, Zeng AP (2007) Metabolic peculiarities of *Aspergillus niger* disclosed by comparative metabolic genomics. Genome Biol 8:R182
Tarze A, Deniaud A, Bras ML, Maillier E, Molle D, Larochette N, Zamzami N, Jan G, Kroemer G, Brenner C (2007) GAPDH, a novel regulator of the pro-apoptotic mitochondrial membrane permeabilization. Oncogene 26:2606–2620
van Leeuwen MRV, Krijgsheld P, Bleichrodt R, Menke H, Stam H, Stark J, Wösten HAB, Dijksterhuis J (2013) Germination of conidia of *Aspergillus niger*, is accompanied by major changes in RNA profiles. Stud Mycol 74:59–70
Waditee R, Hossain GS, Tanaka Y, Nakamura T, Shikata M, Takano J, Takabe T, Takabe T (2004) Isolation and functional characterization of Ca2+/H+ antiporters from cyanobacteria. J Biol Chem 279:4330–4338
Wang B, Guo GW, Wang C, Lin Y, Wang XN, Zhao MM, GuoY He MH, Zhang Y, Pan L (2010) Survey of the transcriptome of *Aspergillus oryzae* via massively parallel mRNA sequencing. Nuleic Acids Res 38:5075–5087
Wang ZL, Zhang LB, Ying SH, Feng MG (2013) Catalases play differentiated roles in the adaptation of a fungal entomopathogen to environmental stresses. Environ Microbiol 15:409–418
Xie XQ, Wang J, Huang BF, Ying SH, Feng MG (2010a) A new manganese superoxide dismutase identified from *Beauveria bassiana* enhances virulence and stress tolerance when overexpressed in the fungal pathogen. Appl Microbiol Biotechnol 86:1543–1553
Xie XQ, Ying SH, Feng MG (2010b) Characterization of a new Cu/Zn-superoxide dismutase from *Beauveria bassiana* and two site-directed mutations crucial to its antioxidation activity without chaperon. Enzyme Microbiol Technol 46:217–222
Yin WB, Reinke AW, Szilágyi M, Emri T, Chiang YM, Keating AE, Pócsi I, Wang CCC, Keller NP (2013) bZIP transcription factors affecting secondary metabolism, sexual development and stress responses in *Aspergillus nidulans*. Microbiol 159:77–88
Yuan XL, Kaaij RMVD, Cees AMJJ, van den Hondel Punt PJ, van der Marc JEC, Maarel Dijkhuizen L, Ram AFJ (2008) *Aspergillus niger*, genome-wide analysis reveals a large number of novel alpha-glucan acting enzymes with unexpected expression profiles. Mol Genet Genomics 279:545–561
Zhang R, Zhao M, Ji HJ, Yuan YH, Chen NH (2013) Study on the dynamic changes in synaptic vesicle-associated protein and axonal transport protein combined with LPS neuroinflammation model. ISRN Neurol 2:496079